A&A manuscript no.
(will be inserted by hand later)

Your thesaurus codes are:
03(04.03.1; 04.19.1; 09.04.1; 11.04.1; 11.03.4; 12.12.1)

ASTRONOMY AND ASTROPHYSICS

Extragalactic large-scale structures behind the southern Milky Way. – III. Redshifts obtained at the SAAO in the Great Attractor region ⋆

Patrick A. Woudt[1], **Renée C. Kraan-Korteweg**[2], **and Anthony P. Fairall**[3]

[1] European Southern Observatory, Karl-Schwarzschildstr. 2, D-85748 Garching, Germany
[2] Departemento de Astronomía, Universidad de Guanajuato, Apartado Postal 144, Guanajuato, Gto 36000, Mexico
[3] Department of Astronomy, University of Cape Town, Rondebosch 7700, South Africa

5 March 1999 / 8 October 1999

Abstract. In the third of a series of papers on large-scale structures behind the southern Milky Way, we report here on redshifts obtained at the South African Astronomical Observatory (SAAO) in the Great Attractor region ($318° \lesssim \ell \lesssim 340°, |b| \leq 10°$, Woudt 1998).

This region encompasses the peak in the reconstructed mass density field, associated with the Great Attractor (Kolatt et al. 1995, Dekel et al. 1998) and covers the crossing of the Supergalactic Plane with the Galactic Plane.

Our deep optical galaxy search in the Zone of Avoidance (ZOA) in this region (Woudt 1998) has resulted in the detection of 4423 galaxies with observed diameters larger than 0.2 arcmin. We have obtained reliable redshifts for 309 galaxies of the 4423 galaxies with the "Unit" spectrograph (first with a Reticon, then with a CCD detector) at the 1.9-m telescope of the SAAO. An additional 13 tentative redshifts are presented. Before our survey, 127 galaxies had a previously recorded redshift (NED and SRC96). Given a small overlap with the literature (44 galaxies), we present here redshifts for 265 galaxies that had no previous recorded velocity. In addition, we present central velocity dispersion (σ_o) measurements for 34 galaxies in ACO 3627.

It is known that the Great Attractor (GA) region is overdense in galaxies at a redshift-distance of $v \sim 5000$ km s^{-1} (Fairall 1988, Dressler 1991, Visvanathan & Yamada 1996, di Nella et al. 1997). We realise here, however, that the Great Attractor region is dominated by ACO 3627 (hereafter referred to as the Norma cluster), a highly obscured, nearby and massive cluster of galaxies close to the plane of the Milky Way (ℓ, b, v) = (325.3°, –7.2°, 4844 km s^{-1}) (Kraan-Korteweg et al. 1996, Woudt 1998).

Previous redshift surveys in the GA region have failed to gauge the significance of the Norma cluster, primarily due to the diminishing effects of the Galactic foreground extinction on the partially obscured galaxies. In the absence of the obscuring effects of the Milky Way, the Norma cluster would have appeared as prominent as the well-known Coma cluster, but nearer in redshift-space. This cluster most likely marks the bottom of the potential well of the Great Attractor (Woudt 1998).

Key words: Catalogs – Surveys – ISM: dust, extinction – Galaxies: distances & redshifts – clusters: individual: ACO 3627 – large-scale structure of Universe

1. Introduction

In two previous papers, we reported on large-scale structures behind the southern Milky Way in the Hydra–Antlia region (Kraan-Korteweg et al. 1995 - hereafter Paper I) and in the Crux region (Fairall et al. 1998 - hereafter Paper II). In the present paper, the third of this series, we present redshifts of galaxies obtained with the 1.9-m telescope of the SAAO in the Great Attractor (GA) region, a region adjacent to the Crux area (Paper II).

Our deep optical galaxy search in the GA region has resulted in the detection of 4423 galaxies with major diameters larger than 0.2 arcmin. They were identified by visually scanning film copies of the SRC IIIaJ survey under 50 times magnification. Details of the galaxy search are given by Woudt (1998) and the results of the galaxy search will be presented as a catalogue (Woudt & Kraan-Korteweg 1999, hereafter WKK99, in prep.). The search in the GA region covers 16 fields of the SRC Sky Survey, namely F99-100, F135-138, F176-180 and F221-225, covering ∼400 square degrees.

The distribution in Galactic coordinates of the 4423 identified galaxies is shown in Fig. 1. A small fraction of these galaxies had been catalogued before by Lauberts (1982), namely 2.4% (=108 galaxies). The adjacent Crux and Hydra–Antlia regions at lower Galactic longitude are

Send offprint requests to: Patrick A. Woudt (email: pwoudt@eso.org)

⋆ All the tables also available in electronic form. See the Editorial in A&AS 1994, Vol. 103, No.1. Based on observations taken at the South African Astronomical Observatory.

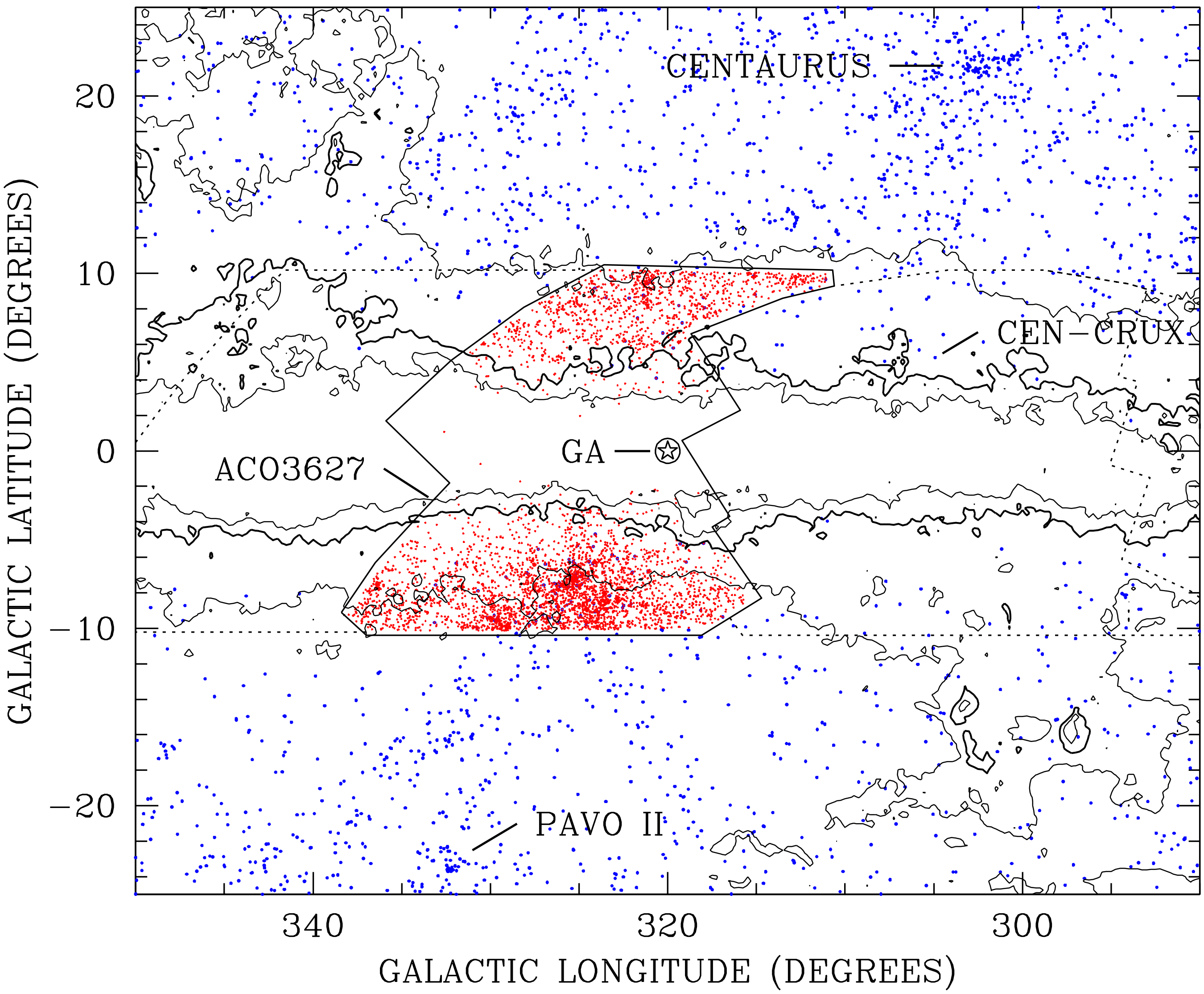

Fig. 1. The distribution of galaxies in the Great Attractor region. The solid line outlines the surveyed area. The galaxies uncovered in the deep optical search ($D \geq 0.2$ arcmin) are displayed as small dots. The larger dots in the surrounding area are the Lauberts galaxies ($D \geq 1.0'$). The Centaurus, Pavo II, Centaurus-Crux and ACO3627 clusters are labelled, as is the location of the peak of the reconstructed mass density field associated with the Great Attractor. The contours are lines of equal Galactic foreground extinction, taken from the Galactic reddening maps of Schlegel et al. (1998). The contours correspond to $A_B = 1^m$, 3^m (thick line) and 5^m.

demarcated by the dotted line in Fig. 1, as is the current extension towards the Galactic Bulge (Fairall & Kraan-Korteweg, in prep.).

By far the most prominent overdensity of galaxies in the GA region is centred on the nearby[1] (cz = 4844 km s^{-1}) Abell cluster ACO 3627 (Abell et al. 1989) at $(\ell, b) \approx (325^\circ, -7^\circ)$ in the constellation of Norma. The galaxies in this overdensity are on average quite large (<D>=30$''\!.$3) and bright (<B_J>=16$^m\!.$9). The large fraction of early type galaxies in ACO 3627 (50% of the galaxies within the core radius are ellipticals or lenticulars) indicate that this is indeed a rich cluster of galaxies. Moreover, if corrected for the obscuring effects of the Galactic extinction (Cameron 1990), and only including galaxies with extinction-corrected diameters $D_0 \geq 1'\!.3$, this region would have the highest galaxy density in the entire southern sky (Woudt 1998).

This clearly suggests that we have unveiled a major cluster of the nearby Universe. The central region of the Norma cluster is a factor $f = 8 - 10$ more dense

[1] To avoid confusion about the redshift-distance of ACO 3627, we quote here the most reliable value as derived from the redshifts of 219 cluster members in the Abell radius (Woudt 1998).

compared to regions at similar Galactic latitude. Due to the diminishing effects of the foreground extinction ($A_B \approx 1^m - 2^m$), the richness of this centrally-condensed cluster had not previously been noticed, even though this cluster lies within 10° of the centre of the Great Attractor $(\ell, b) \approx (320°, 0°)$, *cf.*, Kolatt et al. (1995).

Another significant concentration of galaxies in the GA region is located not far from the Norma cluster, at $(\ell, b) \approx (329°, -9°)$. The relatively large number of early-type galaxies in this overdensity are, on average, much smaller than the early-type galaxies in the Norma cluster, especially when taking into account that the Galactic foreground extinction is nearly identical for both clusters. This overdensity, hereafter referred to as the Ara cluster, is possibly connected to the X-ray bright, and distant Triangulum-Australis cluster at $(\ell, b, v) = (324°,\ -12°,\ 15300$ km s^{-1}) (McHardy et al. 1981).

Hardly any galaxies are visible at extinction levels of $A_B \geq 5$ mag. Our deep optical galaxy search in the Great Attractor region has reduced the optical 'Zone of Avoidance' to Galactic latitudes $|\,b\,| \leq 3°$.

2. Observations

As before in the Hydra–Antlia and Crux regions, we have aimed to be as complete as possible in tracing the bright end of the magnitude distribution of the identified galaxies in the GA region. In addition, particular emphasis is given to the galaxies in the Norma cluster. Together with our MEFOS (Meudon ESO Fibre Optical Spectrograph) observations (Woudt et al. 1999, in prep.) we have aimed to observe all the galaxies down to an extinction-corrected magnitude of $B_J^0 = 15\overset{m}{.}5$, see also Sect. 3.2.

The procedures used for observations at the SAAO are the same as described in Paper I. From the first quarter of 1997 onwards, a new CCD detector has been installed at the 1.9-m telescope of the SAAO, replacing the old Reticon Photon Counting System (RPCS). The RPCS data have been reduced at the University of Cape Town, following the procedure outlined in Paper I. The data obtained with the CCD camera have all been processed by using IRAF[1] and the various tasks within this software package, e.g. *ccdred* and *rvsao*. Both the RPCS and CCD data were taken from March 1994 to May 1997 with grating 7 (210 Å/mm), resulting in a wavelength coverage of 3500 – 7000 Å.

In Table 1[2], the 322 galaxies for which we obtained a redshift at the SAAO are listed. This table includes the 13 tentative redshifts, and the galaxies observed at higher spectral resolution (see Sect. 2.1). The entries in Table 1 are as follows:

Column 1 and 2: Identification of the galaxy as given in WKK99 and Lauberts Identification (Lauberts, 1982).

Column 3 and 4: Right Ascension and Declination (1950.0). The positions were measured with the Optronics machine at the ESO in Garching and have an accuracy of about 1 arcsec.

Column 5 and 6: Galactic longitude ℓ and latitude b.

Column 7: Major and minor axes (in arcsec). These diameters are measured approximately to the isophote of 24.5 mag arcsec^{-2} and have a scatter of $\sigma \approx 4''$.

Column 8: Apparent magnitude B_J. The magnitudes are estimates from the film copies of the SRC IIIaJ Survey based on the above given diameters and an estimate of the average surface brightness of the galaxy.

Column 9: Morphological type. The morphological types are coded similarly to the precepts of the Second Reference Catalogue (de Vaucouleurs et al. 1976). Due to the varying foreground extinction a homogeneous and detailed type classification could not always be accomplished and some codes were added: In the first column F for E/S0 was added to the normal designations of E, L, S and I. In the fourth column the subtypes E, M and L are introduced next to the general subtypes 0 to 9. They stand for early spiral (S0/a-Sab), middle spiral (Sb-Sd) and late spiral or irregular (Sdm-Im). The cruder subtypes are a direct indication of the fewer details visible in the obscured galaxy image. The question mark at the end marks uncertainty of the main type, the colon uncertainty in the subtype.

Column 10: Heliocentric velocity (cz) and error as derived from the absorption features. The errors may appear large as they are estimated external errors, and not internal errors (see Paper I). The square brackets indicate a tentative redshift.

Column 11: Heliocentric velocity and error measured from the emission lines (identified in column 12) when present. The square brackets indicate a tentative redshift.

Column 12: Identified emission lines:

1	2	3	4	5	6	7
[OII]	Hγ	Hβ	[OIII]	[OIII]	Hα	[NII]
3727	4340	4861	4959	5007	6563	6584

Column 13: Code for additional remarks:

$*$ – Redshifts are also available in the literature.

1 – WKK 4001: The redshift measured at the SAAO for this galaxy ($v = 5937 \pm 250$ km s^{-1}) is in disagreement with the value quoted in the literature ($v = 4700 \pm 100$ km s^{-1}, Fairall 1981).

[1] IRAF (Image Reduction and Analysis Facility) is distributed by the National Optical Astronomy Observatories, which are operated by the Association of Universities for Research in Astronomy, Inc., under cooperative agreement with the National Science Foundation

[2] All the tables are only available in electronic form at the CDS via anonymous ftp to cdsarc.u-strasbg.fr (130.79.128.5) or via http://cdsweb.u-strasbg.fr/Abstract.html

2 – WKK 5792: The redshift measured at the SAAO for this galaxy ($v = 13487 \pm 101$ km s^{-1}) is in disagreement with the value quoted in the literature ($v = 3500 \pm 70$ km s^{-1}, di Nella et al. 1997). There is a positional mismatch of 1.1 arcminutes between WKK 5792 and the galaxy quoted by di Nella et al. (1997). However, after visual re-examination, no galaxy is seen on the IIIaJ Sky Survey at the position of di Nella's galaxy and we believe that this velocity should not be trusted.

3 – WKK 6180 / 6212: The redshifts measured for WKK 6180 and WKK 6212 ($v = 4619 \pm 127$ km s^{-1} and 3196 ± 95 km s^{-1}, respectively) are in disagreement with the value quoted in the literature ($v = 3100$ km s^{-1} and $v = 4911$ km s^{-1}, respectively, West et al. 1981). This might be due to an identification error.

4 – WKK 7055: The spectrum is contaminated by the light of a Galactic foreground star. However, a reliable redshift could be obtained.

GR6 – These galaxies have been observed at higher spectral resolution with grating 6 (100 Å/mm), see also Sect. 2.1.

Sy1 – This galaxy, WKK 6092, has been classified as Seyfert 1 (Woudt et al. 1998).

Table 2 [1] lists 22 galaxies for which no redshift could be determined. These spectra either had a poor signal-to-noise ratio or were dominated by the light of a Galactic foreground star.

Table 3 [1] gives redshifts extracted from the literature for 82 galaxies we have not observed in the Great Attractor region. These galaxies would have been included in our observations were they not observed before, since they meet our selection criteria.

Columns 1-9 are the same as in Table 1. Column 10 list the heliocentric velocities and errors (if given). The velocity in column 10 has been adopted from the source identified in column 11, where the number corresponds to:

1. Dressler 1991
2. di Nella et al. 1997
3. Fisher et al. 1995
4. Coté et al. 1997
5. Strauss et al. 1992
6. Jones & McAdam 1992
7. Huchtmeier & Richter 1989
8. Webster 1979
9. Visvanathan & Yamada 1996
10. Mould et al. 1991
11. Fairall 1988
12. Davies et al. 1989
13. Fairall 1983
14. Schmidt & Boller 1992
15. Fairall 1981
16. Whiteoak & Gardner 1977
17. Corwin & Emerson, 1982

2.1. Velocity dispersion measurements for galaxies in the Norma cluster

During one week in April 1996, we observed 39 galaxies in the Norma cluster at higher spectral resolution, *i.e.*, with grating 6 (100 Å/mm = 1.4 Å/pixel) in combination with the RPCS. These galaxies had been observed before, either by us in the course of our redshift survey (34 galaxies), or by others (5 galaxies). The higher spectral resolution allows the determination of the central velocity dispersion of these galaxies. The wavelength coverage ranges from 4100 Å to 6050 Å, i.e. approximately centred on the Mg b absorption lines at $\lambda_0 = 5172$ Å. The slit width is 1.8 arcsec and the length of each slit segment is 6 arcsec. The spectral resolution is approximately 2.9 Å. This was measured from the width of the lines of the calibration lamp, and from the width of the peak of the autocorrelation function of the velocity standard stars. The typical exposure times range between 1500-s and 2000-s per galaxy.

Three standard stars of spectral type G8 to K2 were observed to serve as templates for the velocity dispersion determination. We have used the Tonry & Davis (1979) cross-correlation technique, implemented in the IRAF task *fxcor*, to determine the central velocity dispersion. Scodeggio et al. (1998) reported that *fxcor* overestimates the velocity dispersion at a 5% level, so a small correction needs to be applied to the measured velocity dispersion.

One galaxy, WKK6080, only revealed [OIII] and Hβ in emission, and hence no velocity dispersion measurement could be made for this galaxy. For four further spectra (WKK5919, WKK6221, WKK6298 and WKK6580) no reliable velocity dispersion could be determined because of low signal-to-noise ratios.

Table 4 [1] lists the final 34 galaxies and their respective central velocity dispersion. The entries in Table 1 are:

Column 1 – 8: As in Table 1.
Column 9: The Galactic reddening at the position of each galaxy, taken from the Galactic reddening maps of Schlegel et al. (1998).
Column 10: As Column 9 of Table 1.
Column 11: As Column 10 of Table 1.
Column 12: The measured central velocity dispersion. In brackets, the number of standard stars are given that were used for the determination of the velocity dispersion. A correction is applied to the velocity dispersion following Scodeggio et al. (1998), since the IRAF

[1] All the tables are only available in electronic form at the CDS via anonymous ftp to cdsarc.u-strasbg.fr (130.79.128.5) or via http://cdsweb.u-strasbg.fr/Abstract.html

task *fxcor* overestimates the velocity dispersion at a 5% level.

Column 13: The logarithm of the aperture-corrected (Davies et al. 1987) central velocity dispersion, and its uncertainty calculated from the signal-to-noise ratio of the spectra (Scodeggio et al. 1998).

2.2. Comparison to other measurements

In the course of this redshift survey, some galaxies in our search area have been observed spectroscopically by others (Visvanathan & Yamada 1996, di Nella et al. 1997). Although the galaxies we observed were initially selected on the basis of having no published redshifts, a small overlap now exists.

This overlap allows for a comparison between our sample and others. We find

$$< v_{\rm SAAO} - v_{\rm pub} >= +38 \pm 151 \text{ km s}^{-1}.$$

which shows no significant systematic error, and agrees well within our average standard deviation. This is based on 43 galaxies for which a redshift estimate exists in the literature (not including WKK 4001 and WKK 5792).

Similarly, we have allowed a small overlap between the SAAO galaxies and our complementary programmes using MEFOS and Parkes radio observations (Kraan-Korteweg et al. 1994), for which we find

$$< v_{\rm SAAO} - v_{\rm MEFOS} >= +3 \pm 148 \text{ km s}^{-1},$$

$$< v_{\rm SAAO} - v_{\rm Parkes} >= -10 \pm 238 \text{ km s}^{-1}.$$

The comparison with the MEFOS and Parkes data is based on 24 and 8 galaxies, respectively. The agreement is good. The comparison with Parkes redshifts are mainly for low surface-brightness galaxies, for which our errors are larger.

Note that in some cases, the difference between the optical and HI-based radial velocity is real due to the net outflow of gas in the narrow emission line regions, as for instance in the case of Seyfert galaxies (Mirabel & Wilson 1984). One such galaxy, a Seyfert 1 in ACO 3627 (WKK 6092, see Woudt et al. 1998), has been included in the above statistics. If this galaxy is excluded, we find

$$< v_{\rm SAAO} - v_{\rm Parkes} >= +35 \pm 218 \text{ km s}^{-1}.$$

A final comparison is made for galaxies reobserved at the SAAO at higher spectral resolution with grating 6. All these galaxies are bona fide members of the Norma cluster. Eleven galaxies were observed before with MEFOS on the 3.6-m telescope of ESO, La Silla. For these galaxies we find no significant offset, and a very small standard deviation which reflects the high signal-to-noise ratio at higher spectral resolution for their velocity dispersion determination.

$$< v_{\rm SAAO,\ gr.6} - v_{\rm MEFOS} >= +17 \pm 49 \text{ km s}^{-1}.$$

For 23 of these galaxies, both a low and high spectral resolution spectrum are available from our SAAO data. For these galaxies we find

$$< v_{\rm SAAO,\ gr.6} - v_{\rm SAAO} >= +28 \pm 136 \text{ km s}^{-1}.$$

There are only a few elliptical and lenticular galaxies in the Zone of Avoidance for which the central velocity dispersion has been measured. Dressler et al. (1991) presented data for the three brightest galaxies in the Norma cluster. These galaxies (WKK6269 – the central cD galaxy, WKK6312 – another cD galaxy, and WKK6318 – a bright elliptical galaxy) are also part of our sample of 34 galaxies.

It is difficult to make a quantitative comparison based on this small overlap. Moreover, the three galaxies in common are biased in the sense that they are the brightest ellipticals in the Norma cluster. For these three galaxies we find

$$< \log{(\sigma_{\rm o})}_{\rm SAAO} - \log{(\sigma_{\rm o})}_{\rm lit} >= +0.109 \pm 0.074.$$

Note that one galaxy (WKK6269) is in perfect agreement with Dressler et al. (1991), but that WKK6312 and WKK6318 have a larger dispersion compared to those presented by Dressler et al. (1991). Although we measure a larger velocity dispersion for WKK6312 and WKK6318, these are not atypical values for a cD galaxy, and a bright elliptical galaxy, respectively.

A very recent paper by Lucey et al. (1999, in prep.) reports on velocity dispersion measurements of galaxies in ACO 3627. For six galaxies with sufficiently high signal-to-noise ratio we find a good agreement between the two data sets,

$$< \log{(\sigma_{\rm o})}_{\rm SAAO} - \log{(\sigma_{\rm o})}_{\rm Lucey} >= -0.002 \pm 0.085.$$

3. Coverage and Completeness

3.1. The GA region

The top panel in Fig. 2 shows the distribution in Galactic coordinates of the newly identified galaxies in the GA region. The contours mark the Galactic foreground extinction (Schlegel et al. 1998). The bottom panel of Fig. 2 shows the sky coverage of galaxies with reliable redshifts, indicated by the solid circles. The open circles correspond to galaxies with previously known redshifts. It is clear that a large fraction of our observational effort was directed towards obtaining a fairly complete coverage of the Norma cluster.

3.2. ACO 3627: The Norma cluster

A more detailed view of the sky coverage of galaxies with reliable redshifts in the immediate vicinity of the Norma cluster is shown in Fig. 3.

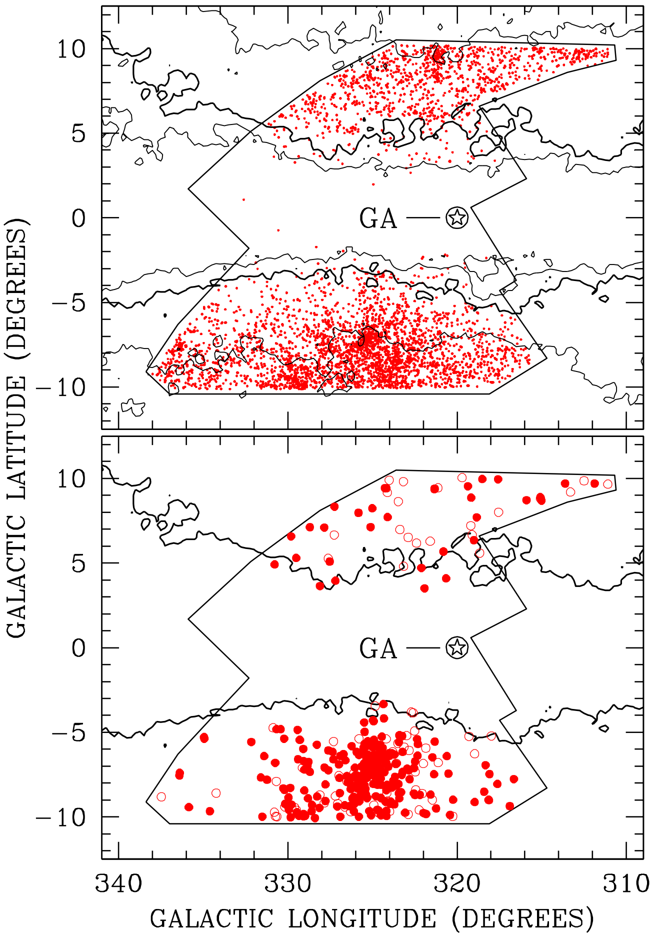

Fig. 2. The top panel shows the distribution in Galactic coordinates of the partially obscured galaxies in the Great Attractor region. The displayed contours mark the foreground extinction (Schlegel et al. 1998), see Fig. 1. The thick line (also shown in the bottom panel) corresponds to $A_{\rm B} = 3\overset{m}{.}0$, below this line our deep optical galaxy survey is not complete anymore for galaxies with $D^0 \geq 1\overset{\prime}{.}3$. The bottom panel shows the distribution of the galaxies with radial velocities. The GA survey region is outlined. Solid circles indicate the positions of galaxies, in the GA region, observed in the present work, and for which redshifts have been obtained. Open circles show the positions of galaxies for which redshifts are available from the literature.

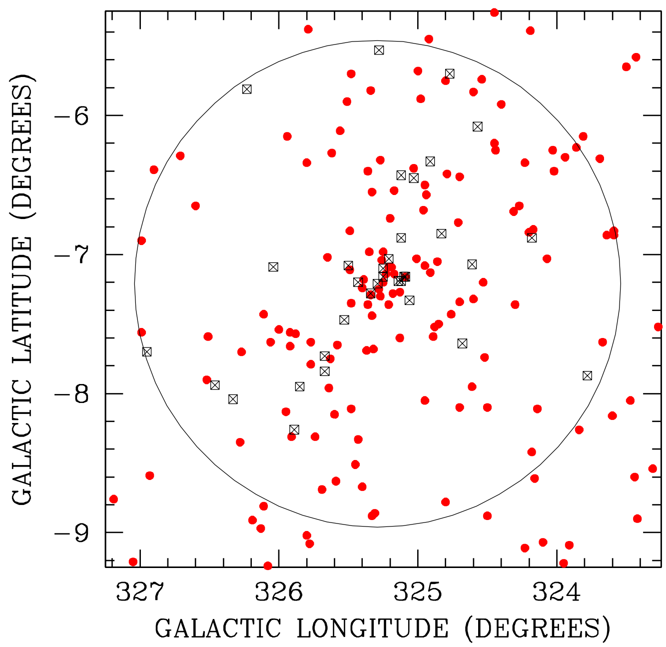

Fig. 3. The distribution of the galaxies with radial velocities in the immediate vicinity of the Norma cluster. The crossed squares are the galaxies for which we have obtained a central velocity dispersion. The filled circles correspond to the galaxies with a reliable redshift (both the newly obtained SAAO redshifts as well as the literature data). The circle marks the Abell radius of the Norma cluster (3 h_{50}^{-1} Mpc, or 1.75 degrees on the sky at the redshift-distance of the Norma cluster).

The filled circles in Fig. 3 correspond to all the galaxies with a known redshift (SAAO and literature data), whereas the crossed squares in Fig. 3 show the 34 galaxies for which we have obtained the central velocity dispersion. The latter sample is spread fairly uniformly over the entire cluster and represents a fair subsample of the Norma cluster. It has a mean velocity of 4877 km s^{-1} and a dispersion of 791 km s^{-1}, compared to 4844 $\pm$ 63 km s^{-1} and 848 km s^{-1} of all Norma cluster members (Woudt 1998).

Apart from our standard observing strategy, *i.e.*, to obtain a spatially uniform coverage of the bright end of the luminosity distribution of the newly catalogued galaxies in the GA region (see also papers I and II), we have aimed to observe all the galaxies brighter than $B_J^0 = 15\overset{m}{.}5$ within the Abell radius of the Norma cluster.

The top panels of Fig. 4 show the magnitude and major-axis distribution of all the galaxies in the Great Attractor region with a reliable redshift. The SAAO data are indicated by the lighter hatched histogram, the dark shaded histogram shows the literature data.

We have achieved a similar completeness compared to the Hydra–Antlia and Crux regions Paper I and II). We are 91% complete for galaxies brighter than ($B_J \leq 14^m$) and even 56% complete for galaxies brighter than ($B_J \leq 16^m$).

The lower panels of Fig. 4 show the *extinction-corrected* magnitude and major-axis distribution of the 603 galaxies within the Abell radius of the Norma cluster (open histogram). Together with data from our MEFOS and Parkes redshift survey, and with literature data, we have now obtained a reliable redshift for 83% of the galaxies with $B_J^0 = 15\overset{m}{.}5$ within 3 Mpc of the Norma cluster. This is illustrated by the cross-hatched histogram in

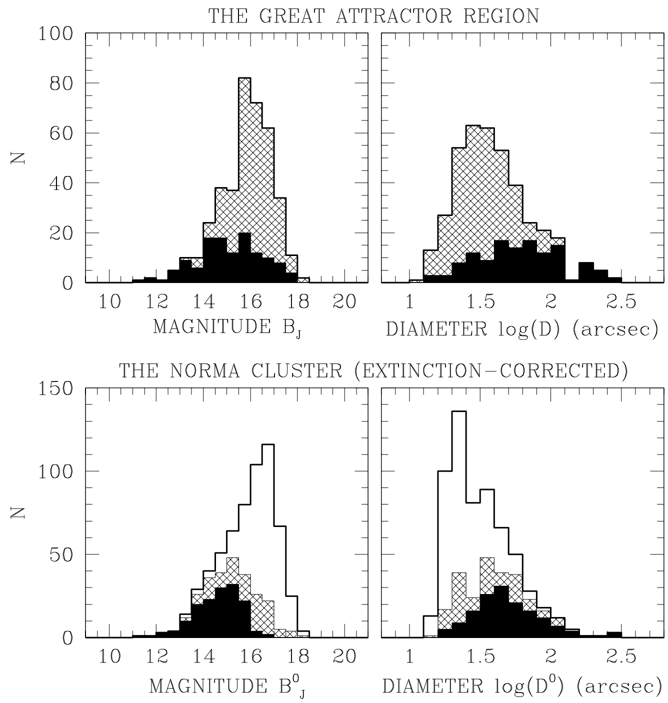

Fig. 4. The top panel shows the magnitude and major-axis distribution of galaxies with radial velocities in the GA region. The lighter hatched areas mark the galaxies observed at the SAAO, the dark shaded histogram are galaxies previously observed by others. The lower panel shows the extinction-corrected magnitude and major-axis distribution of the galaxies in the Norma cluster. The open histograms mark all the optically identified galaxies, the cross-hatched histograms illustrate those galaxies that now have a reliable redshift (including MEFOS, Parkes and literature data) and the dark shaded histograms show the redshifts presented in this paper.

the lower panels of Fig. 4. For the remaining 36 galaxies (=17%) brighter than $B^0_J = 15\overset{m}{.}5$ without redshifts, we have observed a further 10 galaxies, but no reliable redshift could be obtained. For galaxies brighter than $B^0_J = 14\overset{m}{.}5$, 95% of the galaxies were observed and a reliable redshift has been obtained for 91%.

The redshifts obtained at the SAAO (dark shaded histogram in the lower panels of Fig. 4) account for more than 50% of the newly obtained redshifts within the Norma cluster.

4. Identification of Large-Scale Structures

4.1. Velocity distribution

Fig. 5 shows the redshift distribution of the observed galaxies in the GA region. The literature data reveal shallow peaks at 3000 km s^{-1} and 5000 km s^{-1}. With the new redshifts, the peak at 5000 km s^{-1} is the most dominant feature in the GA region. Most of the galaxies at this

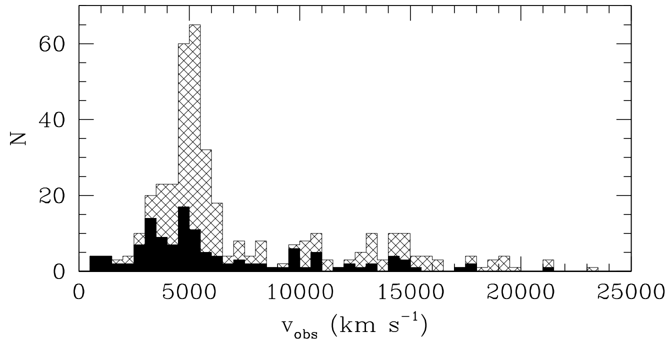

Fig. 5. Velocity histogram of the galaxies in the search area in the Great Attractor extension in the ZOA. Lighter hatched areas are velocities measured by us; darker hatched by others.

redshift-distance belong to the Norma cluster (see Fig. 6), and its immediate surrounding. A more distant (broad) peak can be seen at 15000 km s^{-1}. This peak is associated with the Ara cluster.

In Fig. 6, only the galaxies within the Abell radius of the Norma cluster (the circle in Fig. 3) are plotted. From this velocity histogram it is clear that

- The strong peak at 5000 km s^{-1} in Fig. 5 is primarily due to the Norma cluster.
- The Norma cluster has a large velocity dispersion of $\sigma = 845$ km s^{-1}. This large velocity dispersion is indicative of a very massive cluster. According to the Virial theorem and following Sarazin (1986), it translates into a dynamical mass of 1×10^{15} $M_\odot$ within a 3 h_{50}^{-1} Mpc radius (see also Kraan-Korteweg et al. 1996). The dynamical mass could not have been determined on the basis of the available literature data (20 galaxies, dark shaded histogram in Fig. 6).
- Fore- and background galaxies are clearly offset from the main cluster members. There is hardly any contamination by field galaxies at the cluster core. There are 152 redshifts known within the Abell radius of the Norma cluster, and 137 galaxies (=90%) are cluster members.

Therefore, from the SAAO data alone, one can conclude that the Norma cluster is a massive cluster near the heart of the Great Attractor.

4.2. Sky projection

Before examining the redshift distribution in the sky projection shown here, the reader should be aware that the galaxies plotted in any of the subsequent diagrams constitute an 'uncontrolled' sample of galaxies. The complementary data adjacent to our survey region are taken from the 1996 Southern Redshift Catalogue (SRC) (Fairall 1996) which lists galaxies purely on the basis of them having redshifts.

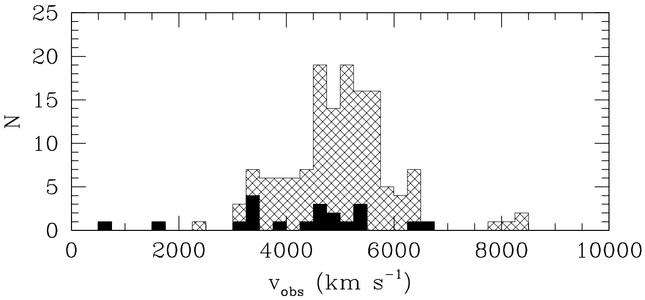

Fig. 6. Velocity histogram of the galaxies within the Abell radius of the Norma cluster. Lighter hatched areas are velocities measured by us at the SAAO; darker hatched by others.

In Fig. 7, we have plotted the galaxy distribution in Galactic coordinates sliced in redshift intervals of $\Delta v = 2000$ km s^{-1} out to 16000 km s^{-1}. The most conspicuous features occur in the second, third and eight slice, coinciding with the peaks observed in the velocity histograms (see Fig. 5). This figure covers the same region of the sky as Fig. 1, where the major concentrations of galaxies are labelled.

In the first slice ($v \leq 2000$ km s^{-1}), the Supergalactic Plane dominates the graph. Our GA search region fully covers the crossing of the Supergalactic Plane with the Galactic Plane. An excess of galaxies is seen within the Supergalactic Plane near the Centaurus A group (at $\ell = 310°$ and $b = 19°$). At higher Galactic longitudes ($340° \leq \ell \leq 360°$), the Local Void is quite distinct.

In the second slice ($2000 \leq v \leq 4000$ km s^{-1}), the new data clearly suggest the presence of a narrow filamentary structure running from $\ell = 340°$, $b = -25°$ to the Centaurus cluster at $\ell = 303°$, $b = 20°$. In Paper II, we already noticed the extension of this structure at low Galactic latitude northwards of the Galactic Plane. Here, we can clearly identify the continuation of this structure below the Galactic Plane, from where it continues to $(\ell, b) = (340°, -25°)$. This extended overdensity is part of a Great Wall-like structure seen edge-on – the Centaurus Wall (Fairall 1998).

The Norma cluster becomes very pronounced in the third redshift slice ($4000 \leq v \leq 6000$ km s^{-1}). This redshift slice corresponds to the redshift-distance of the Great Attractor overdensity, *i.e.*, ~ 4500 km s^{-1} (Lynden-Bell et al. 1988, Kolatt et al. 1995) and coincides with the strong single peak seen in the velocity histogram of the GA region (Fig. 5). The new data, together with the neighbouring galaxies outside the survey area in an extended region around the Pavo II cluster ($\ell \approx 332°$, $b \approx -23°$) suggest a broad large-scale structure running more or less horizontally across the diagram. There is no clear connection to the Centaurus cluster which is located a lower redshift-distance (*e.g.*, Stein et al. 1997 and references therein). This broad feature, also referred to as the "Norma supercluster", was already noted in Paper II.

Traces can also be seen in the following slice, so the feature is also probably wall-like seen roughly side on – *i.e.*, its width (or depth in Fig. 7) being some 3000 km s^{-1}, and its thickness several hundred km s^{-1} unless much is still hidden by the dense obscuration.

The Norma supercluster is located at a greater distance compared to the Centaurus Wall mentioned above, but must be similarly massive. It includes a cluster/group of galaxies around $(\ell, b, v) = (305.5°, +5.5°, 6214$ km s$^{-1})$ (the Centaurus–Crux cluster, Paper II). The Centaurus–Crux cluster and the Vela overdensity (Kraan-Korteweg & Woudt 1993) at $(\ell, b, v) = (280°, +6°, 6000$ km s$^{-1})$ probably form part of the Norma supercluster.

It is likely that the flow motions that led to the prediction of a Great Attractor originate in fact from the confluence of these two massive structures (the Norma supercluster and the Centaurus Wall), at the intersection of which resides the massive Norma cluster.

Although the rich Norma cluster seems to constitute the bottom of the potential well of the GA, it cannot be excluded that other major features of the GA remain hidden by the Galactic foreground extinction. There are various indications that the strong extragalactic radio source PKS1343-601, located at $(\ell, b, v) = (309.7°, +1.7°, 3872$ km s$^{-1})$, could mark the centre of a highly obscured ($A_B = 12^m$) rich cluster in the GA overdensity (Woudt 1998, Kraan-Korteweg & Woudt 1999). The prospective PKS1343-601 cluster is located in the second slice of Fig. 7, near to the intersection of the Norma supercluster and the Centaurus Wall.

In the last redshift slice ($14000 \leq v \leq 16000$ km s^{-1}) the Ara cluster is seen at $(\ell, b) = (329°, -9°)$. This cluster is located near the X-ray bright Triangulum–Australis cluster at $(\ell, b, v) = (324°, -12°, 15300$ km s$^{-1})$ (McHardy et al. 1981). Together, they might be part a larger structure, *i.e.*, a supercluster.

4.3. Pie diagrams

The redshift cones of Fig. 8 clearly show the impact of our redshift survey on the ZOA. The middle panels in Fig. 8 mark the latitude interval $-10° \leq b \leq 10°$, a region that previously was largely blank now shows clusters, superclusters and voids. In this representation, the ZOA out to $\ell = 340°$ is indiscernible from its unobscured counterpart.

The left panel of Fig. 8 shows the galaxies out to a redshift of 10000 km s^{-1}, whereas the right panel shows the galaxies out to twice that distance. The upper panel includes the Centaurus clusters (Cen30 and Cen45), the lower panel includes the Pavo II cluster. The Norma cluster, at $\ell = 325°$ in the ZOA, is very radially extended, indicative of the massive nature of this cluster. The Centaurus–Crux cluster at $\ell = 305°$ (Paper II) appears as a smaller finger of god. Several voids can be iden-

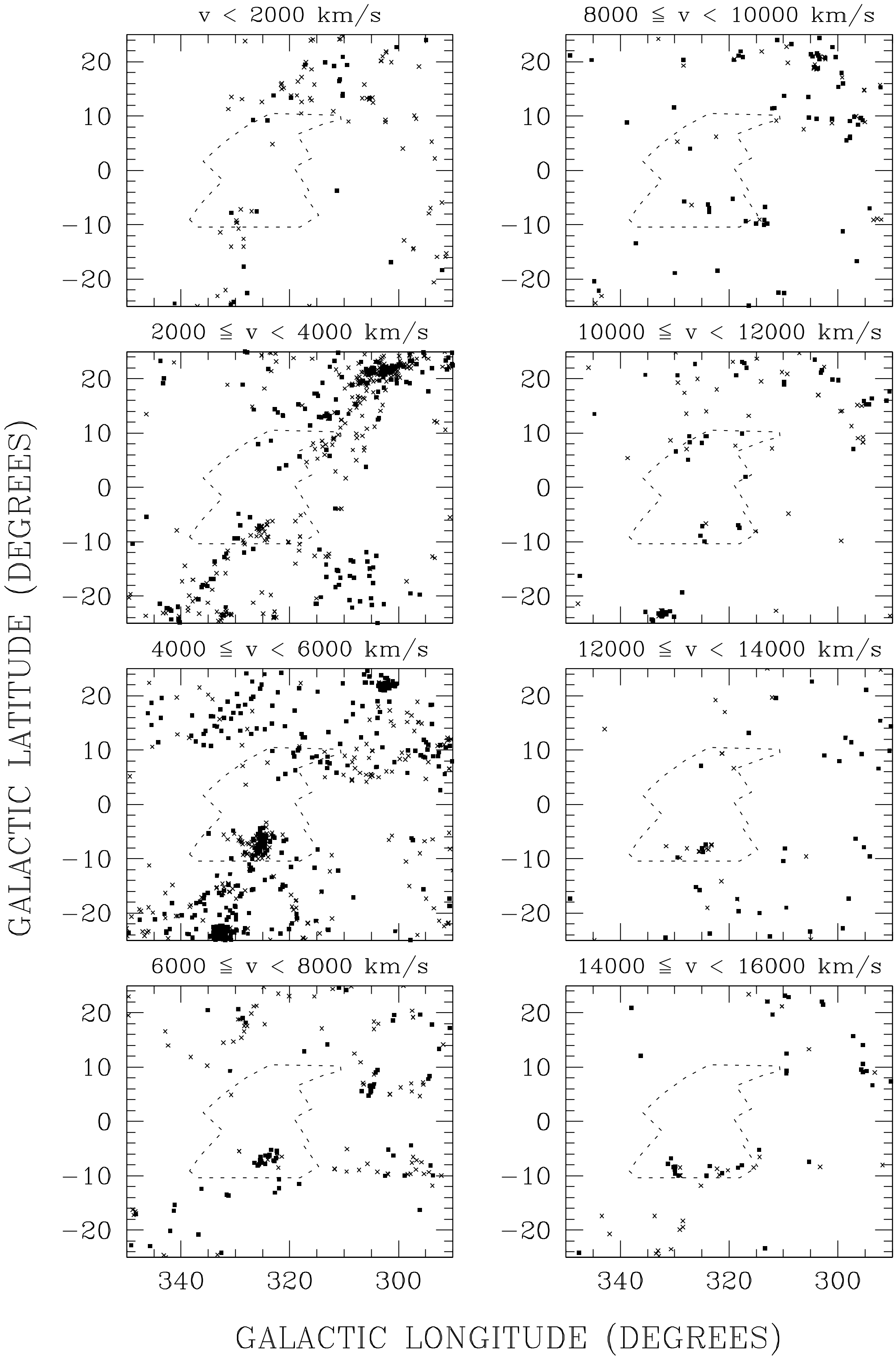

Fig. 7. Sky projections in Galactic coordinates for redshift intervals of $\Delta v = 2000$ km s^{-1}. Within the panels the redshifts are subdivided into intervals of $\Delta v = 1000$ km s^{-1}: filled squares mark the nearer redshift interval (*e.g.*, $v < 1000$ km s^{-1} in the top-left panel), crosses the more distant interval ($1000 \leq v < 2000$ km s^{-1} in same panel). The sky plots increase in velocity-distance from the top-left panel to the bottom-right panel as marked above each panel. The area of our investigation is outlined.

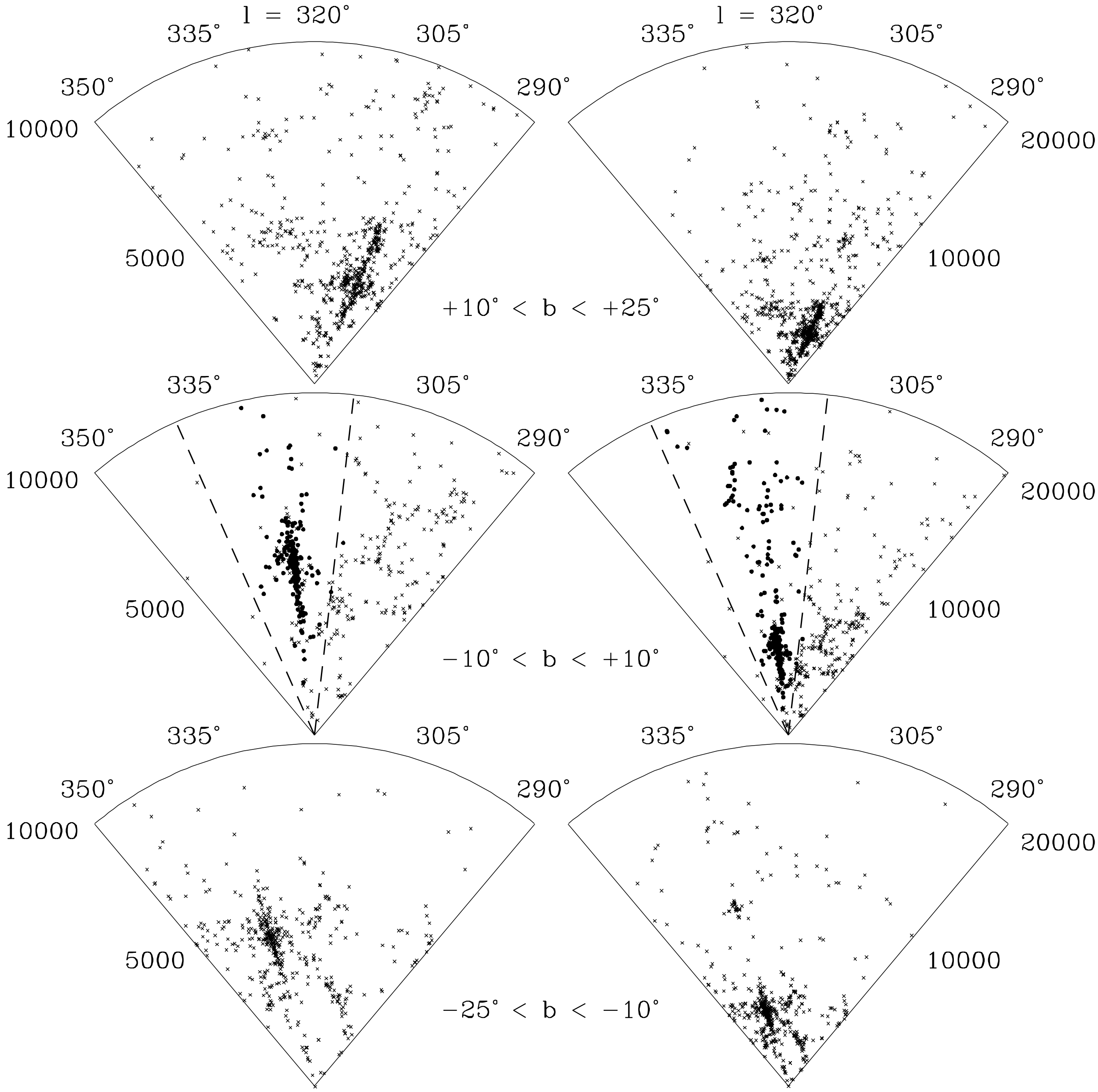

Fig. 8. Redshift slices out to $v < 10000$ km s^{-1} (left panel) and $v < 20000$ km s^{-1} (right panel) for the longitude range $290° < \ell < 350°$. The top panels display the structures above the GP ($+10° < b \leq +25°$) the middle panel in the GP ($-10° \leq b \leq +10°$) and the bottom panel the structures below the GP ($-25° < b \leq -10°$). The dashed lines in the middle panel delimits the survey area. Filled squares are measurements from the SAAO, crosses from the literature.

tified. One of the larger voids in the ZOA is located at $\ell \approx 316°, v \approx 7000$ km s^{-1} and has a radius of $R \approx 1000$ km s^{-1} is the Circinus void (Fairall 1998). It probably connects with the void located behind the GA (da Costa et al. 1996). Further nearby voids can easily be recognised.

5. Summary

Ever since the discovery of the Great Attractor – a massive overdensity partly responsible for the large-scale systematic flow of galaxies in the Local Universe – it was clear that a large fraction of this overdensity was hidden from our view by the obscuring veil of the Milky Way.

Our ZOA redshift survey at the SAAO has resulted in 265 new reliable redshifts in the Great Attractor region. These data clearly show that the Great Attractor region is dominated by a rich and massive cluster at low Galactic latitude, *i.e.*, the Norma cluster.

Moreover, it now emerges that the Great Attractor itself is likely to be the confluence of two massive large-scale structures in this part of the sky, the Centaurus Wall and the partially obscured Norma supercluster.

Acknowledgements. The authors would like to thank the night assistants Francois van Wyk and Fred Marang as well as the staff at the SAAO for their hospitality. We kindly acknowledge John Lucey, who made velocity dispersion measurements of 16 early type galaxies in ACO 3627 available to us before publication. Bruce Bassett assisted APF during the March 1994 observing run. APF is supported by the South African FRD. This research has made use of the NASA/IPAC Extragalactic Database (NED), which is operated by the Jet Propulsion Laboratory, Caltech, under contract with the National Aeronautics and Space Administration.

References

Abell G.O., Corwin H.G., Olowin R.P., 1989, ApJS 70, 1

Cameron L.M. 1990, A&A 233, 16

Corwin H.G., Emerson D. 1982, MNRAS 200, 621

Coté S., Freeman K.C., Carignan C., et al. 1997, AJ 114, 1313

da Costa L.N., Freudling W., Wegner G., et al. 1996, ApJ 468, L5

Davies R.D., Staveley-Smith L., Murray J.D. 1989, MNRAS 236, 171

Davies R.L., Burstein D., Dressler A., et al. 1987, ApJS 64, 581

Dekel A., Eldar A., Kolatt T., et al. 1998, (astro-ph/9812197)

de Vaucouleurs G., de Vaucouleurs A., Corwin H.G. 1976, Second Reference Catalogue of Bright Galaxies (RC2), University of Texas Press, Austin

di Nella H., Couch W.J., Parker Q.A., et al. 1997, MNRAS 287, 472

Dressler A. 1991, ApJS 75, 241

Dressler A., Faber S.M., Burstein D. 1991, ApJ 368, 54

Fairall A.P. 1981, MNRAS 196, 417

Fairall A.P. 1983, MNRAS 203, 47

Fairall A.P. 1988, MNRAS 230, 69

Fairall A.P. 1996, the Southern Redshift Catalogue, maintained at the University of Cape Town (available from fairall@physci.uct.ac.za)

Fairall A.P. 1998, *"Large-Scale Structures in the Universe"*, John Wiley and sons, Praxis and Wiley Publishing, Chichester UK

Fairall A.P., Woudt P.A., Kraan-Korteweg R.C. 1998 (Paper II), A&AS 127, 463

Fisher K.B., Huchra J.P., Strauss M.A., et al. 1995, ApJS 100, 69

Huchtmeier W.K., Richter O.-G. 1989, The General Catalogue of HI-Observations of Galaxies, New York: Springer-Verlag

Jones P.A., McAdam W.B. 1992, ApJS 80, 137

Kolatt T., Dekel A., Lahav O. 1995, MNRAS 275, 797

Kraan-Korteweg R.C., Woudt P.A. 1993, in 9^{th} IAP Astrophysics Meeting on "Cosmic Velocity Fields", eds. F. Bouchet and M. Lachièze-Rey, Editions Frontières, Gif-sur-Yvette, 557

Kraan-Korteweg R.C., Cayatte V., Fairall A.P., et al. 1994, in "Unveiling Large-Scale Structures behind the Milky Way", eds. C. Balkowski and R.C. Kraan-Korteweg, A.S.P. Conf.Ser. 67, 99

Kraan-Korteweg R.C., Fairall A.P., Balkowski C., 1995 (Paper I), A&A 297, 617

Kraan-Korteweg R.C., Woudt P.A., Fairall A.P., et al. 1996, Nature 379, 519

Kraan-Korteweg R.C., Woudt P.A. 1999, PASA 16, 53

Lauberts A. 1982, The ESO/Uppsala Survey of the ESO (B) Atlas, ESO: Garching

Lynden-Bell D., Faber S.M., Burstein D., et al. 1988, ApJ 326, 19

McHardy I.M, Lawrence A., Pye J.P., et al. 1981, MNRAS 197, 893

Mirabel I.F., Wilson A.S. 1984, ApJ 277, 92

Mould J.R., Staveley-Smith L., Schommer R.A., et al. 1991, ApJ 383, 467

Sarazin C.L. 1986, Rev. Mod. Phys. 58, 1

Schlegel D.J., Finkbeiner D.P., Davis M. 1998, ApJ 500, 525

Schmidt K.-H., Boller T. 1992, AN 313, 189

Scodeggio M., Giovanelli R., Haynes M.P. 1998, AJ 116, 2738

Stein P., Jerjen H., Federspiel M. 1997, A&A 327, 952

Strauss M.A., Huchra J.P., Davis M., et al. 1992, ApJS 83, 29

Tonry J.L., Davies R.L. 1979, AJ 84, 1511

Visvanathan N., Yamada T. 1996, ApJS 107, 521

Webster B.L., Goss W.M., Hawarden T.G., et al. 1979, MNRAS 186, 31

West R.M., Surdej J., Schuster H.E., et al. 1981, A&AS 46, 57

Whiteoak J.B., Gardner F.F. 1977, AuJPh 30, 187

Woudt P.A. 1998, Ph.D. thesis, University of Cape Town

Woudt P.A., Kraan-Korteweg R.C., Fairall A.P., et al. 1998, A&A 338, 8

Table 1. Redshifts of partially obscured galaxies in the Great Attractor region obtained at the SAAO.

WKK Ident	Other Ident	R.A. (h m s)	Dec. (° ′ ″)	gal ℓ (°)	gal b (°)	D x d (″)	B_J (^{m})	Type class.	v_{abs} km s^{-1}		v_{em} km s^{-1}		Identified Em. lines	Notes
(1)	(2)	(3)	(4)	(5)	(6)	(7)	(8)	(9)	(10)		(11)		(12)	(13)
WKK3777		13 46 08.0	–51 55 04	311.88	9.70	30x 19	16.8	S E?	9295	250	9226	100	6	*
WKK3814		13 52 21.5	–52 00 21	312.81	9.39	28x 19	17.1	L ?	[19765]	206				
WKK3837		13 56 52.1	–51 30 04	313.62	9.70	24x 8	17.9	S E			5669	50	3 4 5 6	
WKK3891		14 07 13.8	–52 04 53	315.01	8.69	23x 17	16.9	E			3089	41	1 3 4 5 6 7	*
WKK3892		14 07 17.7	–51 51 58	315.09	8.89	19x 16	17.1	E	4200	45				
WKK3915		14 12 33.1	–51 46 46	315.90	8.72	36x 24	16.2	S P			4458	58	3 6 7	*
WKK3959		14 19 53.1	–50 04 13	317.58	9.95	34x 10	17.4	S 1	10842	109				
WKK4001	L222-006	14 25 11.7	–49 43 42	318.51	9.96	87x 32	15.3	S 3	5937	250				1
WKK4079		14 30 59.5	–49 48 05	319.36	9.54	24x 20	17.1	F	4436	53				
WKK4086		14 31 31.0	–50 30 10	319.17	8.86	27x 24	16.8	F	4777	52				
WKK4098		14 32 30.6	–51 42 02	318.84	7.70	31x 20	16.9	S 2	11229	100				
WKK4146		14 36 59.7	–52 52 03	319.01	6.35	52x 35	15.9	S 0 :	4728	130				
WKK4260		14 42 15.5	–49 08 18	321.33	9.40	27x 20	17.0	S 0	13226	70				
WKK4266		14 42 24.6	–49 10 12	321.34	9.36	22x 17	17.3	F	13411	100				
WKK4396		14 49 38.1	–52 42 25	320.81	5.68	20x 12	17.6	E ?	4885	146				
WKK4470	L176-006	14 53 31.8	–54 11 28	320.65	4.10	87x 23	15.6	S M	2869	103				
WKK4539		14 57 17.2	–47 51 00	324.17	9.42	50x 16	16.3	S 0	10243	132	10177	100	6	
WKK4550		14 57 45.2	–47 47 33	324.27	9.43	15x 8	17.9	E	10243	100				
WKK4585	L176-008	15 00 11.6	–52 57 32	322.11	4.72	114x 20	15.7	S 6	4728	137				
WKK4603		15 01 59.2	–49 22 30	324.11	7.71	20x 16	16.9	E	5748	93				
WKK4613		15 03 06.3	–54 06 15	321.93	3.51	23x 13	17.4	S E?			2855	58	3 6 7	
WKK4646		15 05 04.6	–48 28 18	325.01	8.24	34x 17	16.4	L	10400	200				
WKK4711		15 09 00.4	–49 22 47	325.11	7.13	24x 16	17.1	F	12533	225				
WKK4732		15 10 05.9	–48 17 28	325.83	7.97	51x 28	15.5	S P2			2226	45	3 4 5 6 7	
WKK4767		15 12 30.6	–66 29 36	316.65	–7.76	38x 27	16.1	S 3	14915	178				*
WKK4833		15 16 02.7	–47 15 12	327.24	8.33	38x 8	17.4	S 2	10249	250				
WKK4911		15 21 49.7	–64 54 15	318.32	–6.94	40x 26	15.7	S	10520	137				
WKK4914		15 22 12.4	–66 12 44	317.62	–8.05	32x 26	15.8	S	14762	111				
WKK4915		15 22 19.9	–50 28 21	326.35	5.06	13x 10	18.1	E	[10315]	231				
WKK4922		15 22 49.1	–65 28 27	318.09	–7.47	20x 16	16.5	E ?	10645	164	10485	100	6	
WKK4928		15 23 02.5	–47 56 40	327.85	7.10	16x 16	17.2	E	11194	53				
WKK4938	L068-005	15 23 31.5	–67 41 55	316.89	–9.36	63x 27	15.3	L ?	8394	93				
WKK5009		15 27 06.8	–47 27 34	328.70	7.12	30x 23	16.3	S E:			5620	41	1 3 5 6 7	*
WKK5038		15 28 17.4	–49 47 12	327.53	5.09	14x 11	17.8	F	10241	88				
WKK5086		15 30 40.8	–50 54 36	327.19	3.96	31x 11	17.2	S 3 :	8424	104				
WKK5094		15 30 56.9	–66 07 22	318.41	–8.48	47x 13	16.1	S 3 :	[17956]	250				
WKK5095		15 31 01.6	–66 09 03	318.40	–8.51	16x 13	17.2	S E	14998	188				
WKK5104		15 31 42.3	–66 43 01	318.12	–9.01	23x 13	16.4	E ?	3228	113				
WKK5108	L099-007	15 31 46.8	–66 41 42	318.14	–8.99	191x142	12.4	SB 3	3400	122				*
WKK5145		15 34 16.0	–47 15 28	329.81	6.58	16x 7	18.1	E ?	10728	95				
WKK5174		15 36 01.5	–63 09 54	320.61	–6.41	71x 54	14.4	L	4660	108				
WKK5182		15 36 26.4	–50 38 00	328.10	3.65	15x 13	17.4	E			5303	50	3 5 6 7	
WKK5184		15 36 28.7	–62 03 16	321.32	–5.55	50x 20	15.7	L	5174	135				
WKK5198		15 37 20.5	–48 28 06	329.51	5.30	12x 9	18.1	E	9787	121				
WKK5222		15 39 04.0	–66 18 57	318.96	–9.12	73x 56	14.8	S R			4711	50	1 3 6 7	*
WKK5248		15 40 58.6	–64 02 41	320.52	–7.44	20x 12	17.1	L	18910	191				
WKK5270		15 42 14.3	–62 42 09	321.46	–6.47	42x 12	16.2	L	7032	154				
WKK5275		15 42 44.3	–61 18 34	322.36	–5.40	27x 15	16.5	L ?	6010	168				
WKK5308		15 44 00.4	–61 34 06	322.32	–5.70	22x 16	16.4	S E	6559	118				
WKK5326		15 44 46.5	–47 59 33	330.78	4.92	20x 12	17.6	L ?	7226	132				
WKK5339		15 45 09.1	–58 27 26	324.36	–3.34	17x 13	16.7	F	5200	125				
WKK5388		15 47 12.3	–63 33 08	321.37	–7.48	44x 35	15.2	S 1	6643	196	6480	100	6	*
WKK5392		15 47 24.8	–60 37 28	323.24	–5.22	38x 15	16.5	S 1	5180	208				
WKK5398		15 47 39.6	–62 05 10	322.34	–6.38	44x 9	16.0	L	7018	128				
WKK5406		15 47 58.2	–65 25 21	320.24	–8.99	36x 24	16.1	S 0	15041	117				
WKK5413		15 48 16.2	–60 29 10	323.41	–5.18	47x 12	16.0	S 2	6057	174				
WKK5429		15 48 59.9	–59 08 05	324.33	–4.18	39x 20	15.6	L	5024	132				
WKK5470		15 50 29.2	–60 47 17	323.43	–5.58	38x 26	15.8	S 5	5209	214				
WKK5474		15 50 36.8	–62 15 41	322.49	–6.73	39x 17	16.1	S E			6768	58	3 4 5 6	
WKK5515		15 52 14.6	–61 22 02	323.22	–6.16	40x 16	15.8	L	3550	137				
WKK5541		15 52 59.0	–62 31 39	322.54	–7.11	23x 9	17.1	S			7903	58	3 6 7	*
WKK5552		15 53 18.4	–58 48 41	324.97	–4.29	50x 12	15.7	S E	4823	132				
WKK5556		15 53 24.6	–58 52 28	324.93	–4.34	22x 15	16.6	S	4658	162				
WKK5605		15 54 49.0	–65 59 23	320.42	–9.88	62x 56	14.3	S E:	6272	112				*
WKK5615		15 55 09.1	–59 52 53	324.45	–5.26	42x 12	16.5	S M	3993	250	3867	70	1 6	*
WKK5627		15 55 33.4	–64 20 30	321.57	–8.68	22x 16	16.5	S 1 :	18998	213	19009	100	6	
WKK5639		15 55 48.6	–62 25 26	322.85	–7.24	35x 9	16.2	L	6137	122				
WKK5644		15 55 55.1	–62 17 37	322.95	–7.15	24x 11	16.6	L	6230	159				
WKK5648		15 56 00.2	–61 10 32	323.69	–6.31	46x 19	15.7	L	7807	135				
WKK5666		15 56 36.4	–61 00 07	323.86	–6.23	27x 16	16.0	E ?	8429	227				
WKK5679		15 57 04.2	–58 34 19	325.49	–4.42	51x 34	14.8	S E	4018	179				
WKK5703		15 57 46.3	–60 54 44	324.03	–6.25	16x 15	16.7	E	3650	202	3750	100	6	
WKK5718		15 58 12.4	–60 11 22	324.54	–5.74	26x 12	16.7	S E:	5326	150				
WKK5723		15 58 17.6	–60 25 04	324.40	–5.92	36x 12	16.3	S 3 :	4581	142				
WKK5725		15 58 21.8	–65 10 20	321.24	–9.50	34x 11	16.6	L ?	14846	123				
WKK5727		15 58 22.9	–61 39 21	323.59	–6.86	17x 11	16.8	E			4424	58	4 5 6 7	
WKK5730		15 58 29.6	–62 51 21	322.80	–7.77	30x 15	16.6	S 0 :	19061	102				
WKK5733		15 58 31.5	–61 01 48	324.02	–6.40	54x 9	16.4	S 3	6215	92				
WKK5739		15 58 41.3	–61 37 26	323.64	–6.86	44x 19	15.7	S 0 :	8073	218	8090	100	6	
WKK5740		15 58 41.4	–62 15 39	323.22	–7.34	28x 19	15.9	S E?	13248	250	13108	100	6	
WKK5749		15 58 55.7	–59 43 30	324.92	–5.45	22x 11	17.0	S E	5373	250				
WKK5751	L136-013	15 58 59.9	–60 13 10	324.60	–5.83	48x 19	15.3	S E	4984	250				
WKK5764		15 59 20.1	–60 00 40	324.77	–5.70	34x 32	15.1	E	5028	93				GR6
WKK5774		15 59 37.7	–59 00 33	325.46	–4.97	56x 19	15.2	S E	4777	157				
WKK5779		15 59 50.3	–60 01 36	324.80	–5.75	22x 7	17.6	S	5632	250				
WKK5789		16 00 00.2	–63 56 58	322.20	–8.70	19x 15	16.4	E			15199	58	1 3 6 7	
WKK5792		16 00 02.0	–62 21 35	323.27	–7.52	20x 17	16.6	E ?	13487	101				2
WKK5798		16 00 09.9	–60 25 42	324.57	–6.08	39x 24	15.4	F	5426	151				GR6
WKK5805	L136-018	16 00 20.0	–60 38 20	324.44	–6.25	71x 16	15.5	S 5	6207	230				
WKK5812		16 00 36.0	–59 50 44	325.00	–5.68	46x 23	15.6	S E	5133	152				

Table 1. Continued – Redshifts of partially obscured galaxies in the Great Attractor region obtained at the SAAO.

WKK Ident (1)	Other Ident (2)	R.A. (h m s) (3)	Dec. (° ′ ″) (4)	gal ℓ (°) (5)	gal b (°) (6)	D x d (″) (7)	B_J (^{m}) (8)	Type class. (9)	v$_{abs}$ km s^{-1} (10)	v$_{em}$ km s^{-1} (11)	Identified Em. lines (12)	Notes (13)
WKK5835		16 01 28.9	–61 03 00	324.27	–6.65	19x 12	16.8	S	11261 228	11368 50	1 3 5 6	
WKK5836		16 01 29.2	–59 32 45	325.28	–5.53	23x 15	16.3	F	5415 128			GR6
WKK5840		16 01 33.7	–60 00 36	324.98	–5.88	50x 15	15.7	S 1 :	5177 182			
WKK5846		16 01 44.6	–61 14 52	324.17	–6.82	38x 22	15.6	S E	3717 180			
WKK5853		16 01 51.6	–63 38 48	322.56	–8.61	44x 20	15.5	S 1	8225 146			*
WKK5855		16 01 54.2	–61 03 23	324.31	–6.69	50x 34	14.8	S 0	5387 93			
WKK5856	L100-009	16 01 54.5	–63 46 08	322.48	–8.71	78x 24	14.9	S 0 :	3519 83			*
WKK5864		16 02 04.0	–61 14 21	324.20	–6.84	31x 11	16.5	L ?	3598 141			
WKK5868		16 02 09.4	–61 17 11	324.18	–6.88	59x 44	14.5	F	3330 107			GR6
WKK5879		16 02 19.8	–61 28 00	324.07	–7.03	54x 27	15.2	S 5	7838 232			
WKK5899		16 02 56.6	–60 36 49	324.70	–6.44	43x 32	15.2	S 2	5062 162			
WKK5908		16 03 15.5	–62 10 35	323.67	–7.63	30x 17	15.9	E	8481 102			
WKK5912		16 03 20.6	–59 43 35	325.34	–5.82	55x 24	15.1	SY 0	5073 102			
WKK5913		16 03 23.1	–60 32 13	324.79	–6.42	58x 38	14.5	L	4573 118			
WKK5919		16 03 33.2	–59 32 38	325.48	–5.70	34x 15	16.0	E	4310 188			GR6
WKK5920		16 03 35.3	–60 23 13	324.91	–6.33	39x 39	14.9	F	4744 109			GR6
WKK5945		16 04 26.8	–62 37 25	323.47	–8.05	46x 13	16.0	L	8181 143	8096 100	6	*
WKK5949		16 04 30.0	–65 02 00	321.83	–9.83	17x 15	17.0	S E	15945 143			
WKK5951		16 04 30.7	–60 20 46	325.03	–6.38	35x 24	15.8	SBRM		4741 58	3 6 7	
WKK5961		16 04 45.2	–60 29 25	324.95	–6.50	34x 15	16.0	S E	5088 150			
WKK5964		16 04 46.7	–60 51 13	324.71	–6.77	26x 11	16.7	S 0	4915 142			
WKK5963		16 04 46.7	–59 40 01	325.51	–5.90	56x 27	15.1	L	5255 129			
WKK5972		16 04 58.4	–60 23 56	325.03	–6.45	48x 32	14.8	E	5563 85			GR6
WKK5975		16 05 01.5	–60 32 49	324.94	–6.57	32x 8	16.4	E ?	5698 193			
WKK5983		16 05 12.7	–64 52 56	321.99	–9.77	47x 30	15.5	S	14838 178			*
WKK5986		16 05 18.7	–62 16 39	323.78	–7.87	52x 44	14.6	F	5569 188			GR6
WKK5987		16 05 19.5	–60 19 28	325.12	–6.43	34x 32	15.2	E	4842 231			GR6
WKK5995		16 05 37.8	–61 33 29	324.30	–7.36	22x 11	16.6	F	12608 92			
WKK5996		16 05 38.0	–60 08 16	325.27	–6.32	38x 11	16.1	S 0	5230 112			
WKK6006		16 05 47.5	–60 37 16	324.96	–6.68	59x 17	15.3	S M	5644 197			
WKK6012		16 05 51.0	–61 08 10	324.61	–7.07	32x 22	15.8	F	4352 104			GR6
WKK6017		16 05 55.6	–62 36 55	323.60	–8.16	38x 22	16.1	SB 2	14336 223			
WKK6019		16 05 57.3	–60 49 43	324.83	–6.85	54x 22	15.1	F	5615 172			GR6
WKK6026		16 06 06.0	–61 16 51	324.53	–7.20	34x 17	15.9	SY E	4617 167			
WKK6029	L136-022	16 06 13.6	–59 47 14	325.56	–6.11	58x 17	15.6	S 2	5123 112			
WKK6030		16 06 17.0	–60 21 59	325.17	–6.54	38x 11	16.3	L	5547 199			
WKK6034		16 06 19.7	–63 05 14	323.31	–8.54	28x 26	16.4	SYR	17822 147			
WKK6045		16 06 38.5	–60 08 11	325.36	–6.40	28x 19	16.1	L ?	4929 134			
WKK6056		16 06 48.6	–60 22 59	325.21	–6.59	42x 12	15.9	F	[13758] 250			
WKK6075		16 07 14.9	–60 16 30	325.33	–6.55	20x 11	16.7	F	5101 250			
WKK6076		16 07 15.1	–61 19 36	324.60	–7.32	46x 11	15.9	L	4169 127			
WKK6080		16 07 20.7	–60 14 00	325.36	–6.53	26x 12	16.5	F		6729 58	3 4 5	*,GR6
WKK6086		16 07 26.3	–59 52 10	325.62	–6.27	24x 13	16.5	S 1 :	4638 149			
WKK6089		16 07 29.3	–63 02 31	323.44	–8.60	39x 22	15.8	S 0	19647 172			
WKK6092		16 07 32.7	–60 30 11	325.20	–6.74	56x 47	14.7	SB 2		4688 38	1 3 4 5 6 7	Sy1
WKK6116	L136-024	16 07 52.0	–60 39 17	325.12	–6.88	47x 42	14.6	E	3909 208			*,GR6
WKK6118		16 07 55.2	–61 16 27	324.70	–7.34	32x 15	16.0	S 1	4648 150	4804 70	6 7	
WKK6120		16 07 57.6	–60 54 47	324.95	–7.08	26x 13	16.6	S	5508 192			
WKK6123		16 07 59.3	–60 58 56	324.91	–7.13	58x 56	14.7	S R	10542 126	10611 100	6	
WKK6124		16 07 59.6	–62 31 44	323.84	–8.26	36x 9	16.3	L	13949 177			
WKK6131		16 08 03.8	–60 50 28	325.01	–7.03	28x 13	16.3	L	4784 112			
WKK6146		16 08 28.4	–59 06 52	326.23	–5.81	55x 38	14.6	F	5701 112			GR6
WKK6156		16 08 39.4	–59 33 52	325.94	–6.15	19x 9	17.1	S E	5814 250			
WKK6161		16 08 45.8	–61 17 53	324.76	–7.43	44x 20	15.7	L ?	5281 90			
WKK6168		16 08 50.7	–59 47 46	325.80	–6.34	34x 17	15.9	L ?	5242 88			
WKK6173		16 08 57.5	–62 13 04	324.14	–8.11	27x 12	16.6	S E?	13444 98			
WKK6176	L137-001	16 09 07.6	–60 38 13	325.25	–6.98	86x 31	14.6	S 5		4630 58	3 6 7	
WKK6178		16 09 09.8	–61 41 18	324.52	–7.74	47x 15	15.9	S 5	6145 142			
WKK6180		16 09 11.3	–60 52 45	325.09	–7.16	36x 31	15.2	F	4619 127			GR6
WKK6181	L100-013	16 09 12.3	–63 16 49	323.42	–8.90	60x 20	15.0	S E		3308 70	6	*
WKK6183		16 09 12.9	–60 41 46	325.21	–7.03	30x 24	15.6	E	5845 148			GR6
WKK6190	L137-003	16 09 18.5	–60 52 19	325.10	–7.16	27x 17	16.0	F ?	4454 127			GR6
WKK6196		16 09 27.2	–60 45 27	325.19	–7.09	31x 19	16.2	S M	4818 192			
WKK6198		16 09 30.5	–61 30 20	324.68	–7.64	22x 17	16.1	E	4687 182			GR6
WKK6201		16 09 33.4	–60 44 26	325.21	–7.09	60x 16	15.4	L	3007 125			
WKK6202		16 09 33.5	–60 40 12	325.26	–7.04	39x 17	16.1	S ?	3521 149			
WKK6204	L137-003	16 09 35.4	–60 53 04	325.12	–7.19	42x 35	14.9	F	4678 127			3,GR6
WKK6212		16 09 40.0	–60 51 51	325.14	–7.19	28x 19	15.6	E	3196 95			3,GR6
WKK6221		16 09 44.1	–60 22 05	325.49	–6.83	30x 22	15.6	E	5841 250			GR6
WKK6227	L137-005	16 09 45.8	–61 17 17	324.85	–7.50	42x 38	15.3	S M	5968 225			
WKK6228		16 09 46.6	–60 34 18	325.35	–6.98	43x 12	16.0	L	5671 120			
WKK6229		16 09 50.2	–60 43 26	325.25	–7.10	15x 13	16.6	E	5300 132			GR6
WKK6233		16 09 57.6	–60 45 51	325.23	–7.14	13x 11	17.1	E	5055 185			
WKK6235		16 10 00.9	–61 01 04	325.06	–7.33	32x 24	15.6	E	4067 100			GR6
WKK6238		16 10 03.0	–61 16 57	324.88	–7.52	46x 17	15.7	L	3606 222			
WKK6239		16 10 04.2	–60 56 05	325.13	–7.27	51x 28	15.2	S 2	4175 102	4235 45	1 3 5 6 7	
WKK6242		16 10 09.9	–60 46 12	325.25	–7.16	28x 12	16.4	F	5354 250			GR6
WKK6250		16 10 24.0	–60 54 18	325.18	–7.28	36x 16	15.7	L	6258 153			
WKK6251		16 10 24.3	–60 48 03	325.25	–7.20	36x 18	15.9	S 4	5627 231	5689 100	6 7	
WKK6258		16 10 30.4	–61 19 37	324.89	–7.59	32x 27	15.8	L ?	5240 167			
WKK6269	L137-006	16 10 43.0	–60 46 54	325.29	–7.21	90x 63	13.5	c D	5409 151			*,GR6
WKK6282		16 10 54.6	–60 48 44	325.28	–7.25	22x 22	15.9	E	4849 169			
WKK6285		16 10 56.0	–61 46 38	324.61	–7.95	46x 35	15.1	S R	4375 250	4532 100	6	
WKK6290		16 11 02.8	–62 24 59	324.18	–8.42	34x 24	15.8	S 1	4815 140	4779 100	6	
WKK6294		16 11 03.5	–60 56 40	325.21	–7.36	23x 12	16.8	L	4547 191			
WKK6297		16 11 05.9	–60 51 20	325.27	–7.30	24x 19	16.2	S E	5023 220			
WKK6298		16 11 06.4	–61 57 51	324.50	–8.10	46x 11	15.6	F	5130 132			GR6
WKK6299		16 11 08.6	–60 41 26	325.39	–7.18	13x 11	17.4	S	5211 132			
WKK6305	L137-007	16 11 13.0	–60 32 24	325.50	–7.08	59x 44	14.4	E	5038 124			*,GR6
WKK6309		16 11 18.1	–60 34 30	325.49	–7.11	22x 19	16.4	S R ?		6169 70	6 7	

Table 1. Continued – Redshifts of partially obscured galaxies in the Great Attractor region obtained at the SAAO.

WKK Ident (1)	Other Ident (2)	R.A. (h m s) (3)	Dec. (° ′ ″) (4)	gal ℓ (°) (5)	gal b (°) (6)	D x d (″) (7)	B_J (^{m}) (8)	Type class. (9)	v_{abs} km s^{-1} (10)	v_{em} km s^{-1} (11)	Identified Em. lines (12)	Notes (13)
WKK6312	L137-008	16 11 25.2	–60 47 38	325.34	–7.28	110x 95	13.1	cD	3907 132			*,GR6
WKK6313		16 11 25.8	–60 47 54	325.34	–7.29	16x 15	16.7	E ?	3319 104			
WKK6318	L137-010	16 11 29.6	–60 40 41	325.43	–7.20	121x 82	13.2	E	3419 182			*,GR6
WKK6319	L137-011	16 11 32.4	–60 43 29	325.40	–7.24	78x 20	14.9	L P	3877 135			
WKK6329		16 11 45.3	–60 23 24	325.65	–7.02	15x 10	17.3	F	2477 250			
WKK6342		16 11 57.6	–60 49 56	325.36	–7.36	26x 15	16.3	F	4828 203			
WKK6360		16 12 15.2	–60 55 19	325.33	–7.44	36x 27	15.3	E	6258 100			
WKK6363		16 12 17.3	–64 08 08	323.07	–9.75	24x 19	16.3	S 2	12286 243	12096 50	1 3 6 7	*
WKK6366		16 12 21.4	–61 49 39	324.70	–8.10	42x 9	16.4	S 3		3870 58	1 5 6	
WKK6383		16 12 39.3	–60 45 00	325.48	–7.35	34x 19	15.9	L	5431 192			
WKK6415		16 13 15.0	–63 20 21	323.71	–9.26	26x 22	16.0	S 0 ?		13275 58	1 3 6	*
WKK6422		16 13 28.3	–61 37 01	324.95	–8.05	17x 8	17.6	S E?	12998 128			
WKK6423	L100-017	16 13 29.5	–63 04 47	323.91	–9.09	83x 62	13.9	E	3576 115			
WKK6429		16 13 32.1	–61 05 38	325.32	–7.68	27x 15	16.4	L ?	4035 138			
WKK6431		16 13 35.7	–60 48 02	325.53	–7.47	35x 22	15.7	F	3494 124			GR6
WKK6441		16 13 44.0	–59 08 17	326.71	–6.29	20x 15	16.9	L	4523 97			
WKK6451		16 13 54.3	–61 04 23	325.37	–7.69	39x 12	16.4	S 0	4475 157			
WKK6473		16 14 22.5	–60 10 21	326.04	–7.09	17x 11	17.0	E	5561 112			GR6
WKK6479		16 14 28.7	–63 08 36	323.95	–9.22	55x 44	14.4	E	4997 98			*
WKK6493		16 14 42.4	–60 52 18	325.58	–7.62	30x 8	17.0	S 0	[5184] 300			
WKK6503	L137-016	16 14 54.9	–60 53 56	325.58	–7.65	83x 26	14.5	S 0	3939 104			
WKK6512		16 15 04.5	–59 28 37	326.60	–6.65	19x 9	16.9	E		4154 70	6 7	
WKK6524	L137-017	16 15 20.6	–59 04 56	326.90	–6.39	69x 44	14.7	S 5 :	9435 250			
WKK6532		16 15 33.3	–62 52 33	324.23	–9.11	32x 22	15.7	S 1	9840 149			*
WKK6545		16 15 46.1	–62 31 21	324.50	–8.88	30x 13	16.7	S M	4822 202	4849 70	6	
WKK6546		16 15 46.2	–60 55 34	325.63	–7.75	46x 24	15.4	L	4379 223			
WKK6554		16 15 52.1	–60 44 53	325.77	–7.63	27x 17	16.5	S E		4560 70	6 7	
WKK6555		16 15 52.6	–60 53 34	325.67	–7.73	28x 17	16.3	F	4927 167			GR6
WKK6557		16 15 54.4	–58 07 02	327.63	–5.76	26x 10	16.8	S 0		[13023] 100	6	
WKK6575		16 16 13.6	–60 37 41	325.88	–7.57	23x 10	16.8	E	5459 110			
WKK6580		16 16 22.7	–60 35 27	325.92	–7.56	28x 16	16.3	F	5717 182			GR6
WKK6586		16 16 29.3	–60 58 07	325.67	–7.84	46x 33	15.0	F	6389 151			GR6
WKK6592		16 16 35.9	–58 35 38	327.36	–6.16	17x 12	17.4	L	18675 130			
WKK6598		16 16 42.5	–60 31 23	326.00	–7.54	31x 11	16.8	L ?	3860 121			
WKK6602		16 16 48.7	–60 51 58	325.77	–7.79	36x 23	15.7	L	3698 85			
WKK6607		16 16 56.0	–62 14 25	324.80	–8.78	30x 17	16.5	L	12990 144			
WKK6610		16 16 58.4	–60 39 51	325.92	–7.66	98x 66	13.7	L	5182 80			
WKK6615		16 17 02.3	–61 17 36	325.48	–8.11	16x 15	16.9	F	4067 153			
WKK6620		16 17 03.4	–61 03 59	325.64	–7.96	20x 8	17.3	F	6256 148			
WKK6642		16 17 26.2	–58 21 05	327.61	–6.07	20x 16	16.8	S E	23417 150			
WKK6663		16 17 55.9	–61 14 25	325.60	–8.15	85x 20	15.0	S 2		3062 70	6 7	
WKK6666		16 17 57.9	–61 28 52	325.43	–8.33	27x 24	16.0	L	5296 185			
WKK6679		16 18 11.8	–60 55 13	325.85	–7.95	26x 24	15.9	E	4598 103			GR6
WKK6700		16 18 36.5	–63 16 40	324.18	–9.64	36x 17	16.0	S 1		3506 45	1 3 4 5 6 7	
WKK6701		16 18 40.1	–59 22 39	326.99	–6.90	39x 22	15.8	L	5941 122			
WKK6703		16 18 42.3	–58 56 24	327.31	–6.60	26x 12	16.8	S 1	21446 223			
WKK6723	L137-021	16 19 10.0	–61 35 31	325.45	–8.51	101x 19	14.6	S 1	4656 123			
WKK6724		16 19 10.9	–60 26 52	326.27	–7.70	20x 11	16.9	E	5524 150			
WKK6730		16 19 15.6	–57 38 18	328.29	–5.73	22x 13	16.7	L	[8341] 300	8361 70	6 7	
WKK6746		16 19 38.6	–61 14 59	325.74	–8.31	31x 15	16.6	S E	5586 189			
WKK6752		16 19 50.1	–61 44 29	325.40	–8.67	24x 20	16.4	S E	13461 87			
WKK6754		16 19 51.3	–60 58 46	325.95	–8.13	48x 27	15.3	L	6299 110			
WKK6755	CSRG0802	16 19 52.3	–60 11 46	326.51	–7.59	69x 34	14.6	SY E	6326 250			
WKK6765		16 20 15.6	–61 06 17	325.89	–8.26	47x 34	15.0	F	5191 124			GR6
WKK6770		16 20 28.4	–63 30 03	324.17	–9.95	23x 17	16.3	E	14768 117			
WKK6772		16 20 29.7	–61 56 16	325.31	–8.86	15x 8	17.4	E		3894 58	4 5 6 7	
WKK6774		16 20 34.6	–56 12 56	329.43	–4.86	39x 23	16.0	S E		2664 45	3 4 5 6 7	
WKK6778		16 20 37.1	–60 55 34	326.05	–8.16	30x 20	16.1	S 0 ?	[3138] 300			
WKK6779		16 20 39.4	–61 07 55	325.91	–8.31	42x 11	16.4	S 2	5434 133			
WKK6782		16 20 44.5	–61 56 24	325.33	–8.88	36x 15	16.0	S 0	10024 171			
WKK6785		16 20 47.6	–61 34 45	325.59	–8.63	35x 19	16.1	S E	13306 140			
WKK6802		16 21 20.5	–62 56 09	324.65	–9.62	38x 19	15.9	S 1 :		3916 41	1 3 4 5 6 7	*
WKK6803		16 21 23.2	–62 51 04	324.72	–9.57	38x 23	15.5	L	3577 100			*
WKK6808	L137-024	16 21 27.7	–60 38 20	326.33	–8.04	85x 70	13.7	F	5154 167			*,GR6
WKK6821		16 21 38.3	–60 28 46	326.46	–7.94	26x 12	16.4	E	5557 167			GR6
WKK6829	L137-026	16 21 43.1	–61 32 55	325.69	–8.69	82x 27	14.5	S 1	4957 91			
WKK6845		16 22 13.7	–63 14 00	324.50	–9.90	26x 19	16.3	S 1 :	10975 175			
WKK6869		16 22 57.4	–56 43 41	329.29	–5.45	38x 19	16.1	S E		7390 58	3 6 7	
WKK6870		16 22 57.6	–59 57 42	326.95	–7.70	20x 19	16.3	E	5488 148			GR6
WKK6871		16 22 58.2	–56 43 19	329.30	–5.45	32x 11	16.7	S E	7127 151			
WKK6874		16 23 03.3	–60 53 31	326.28	–8.35	38x 20	15.8	S 0	5096 170			
WKK6876		16 23 12.0	–58 48 48	327.81	–6.92	69x 34	14.8	L ?	[14362] 300			
WKK6902		16 23 55.0	–59 10 10	327.61	–7.24	27x 24	16.2	L	5216 250			
WKK6912		16 24 15.9	–58 53 59	327.84	–7.08	38x 17	16.1	L	5337 104			
WKK6915		16 24 18.2	–61 42 06	325.80	–9.02	58x 22	15.2	S 0	4602 108			
WKK6934		16 24 35.1	–61 45 25	325.78	–9.08	42x 12	16.4	S 2	5958 250			
WKK6940		16 24 42.3	–62 34 32	325.19	–9.65	19x 9	17.1	E		9864 45	1 3 4 5 6	*
WKK6942		16 24 43.9	–57 14 42	329.09	–5.98	16x 13	17.1	E	5212 165			
WKK6943		16 24 45.8	–61 19 57	326.11	–8.81	51x 38	14.8	F	4596 126			
WKK6961		16 25 20.8	–55 28 17	330.43	–4.82	26x 17	16.4	F	4666 177			
WKK6976		16 25 38.4	–62 49 08	325.08	–9.90	23x 22	16.2	F	5013 159			
WKK6988		16 25 52.3	–61 20 54	326.19	–8.91	31x 15	16.4	L	5014 145			
WKK7022		16 26 29.5	–55 18 01	330.67	–4.82	31x 13	16.4	S E		4877 50	2 3 6 7	*
WKK7055		16 27 11.7	–56 00 47	330.22	–5.38	58x 26	15.2	S 1	5952 103			4
WKK7061		16 27 17.4	–61 39 08	326.08	–9.24	38x 10	16.5	S 2	16090 199			
WKK7062		16 27 17.8	–57 59 32	328.78	–6.75	70x 56	14.3	F	5252 207			
WKK7079		16 28 03.2	–59 19 39	327.87	–7.73	27x 15	16.6	S	[4383] 225			
WKK7080		16 28 05.0	–60 35 23	326.93	–8.59	22x 15	16.8	S E	18854 101			
WKK7093		16 28 31.5	–57 44 49	329.07	–6.70	50x 38	14.9	F	5120 168			
WKK7098		16 28 46.0	–58 05 51	328.84	–6.96	48x 13	16.0	S 1 :	5238 237			

Table 1. Continued – Redshifts of partially obscured galaxies in the Great Attractor region obtained at the SAAO.

WKK Ident (1)	Other Ident (2)	R.A. (h m s) (3)	Dec. (° ′ ″) (4)	gal ℓ (°) (5)	gal b (°) (6)	D x d (″) (7)	B_J (^{m}) (8)	Type class. (9)	v_{abs} km s^{-1} (10)	v_{em} km s^{-1} (11)	Identified Em. lines (12)	Notes (13)
WKK7105		16 28 56.4	−61 38 56	326.22	−9.39	30x 16	16.1	L	5567 160			
WKK7122		16 29 35.8	−57 26 25	329.40	−6.59	28x 19	16.3	S 0	5368 135			
WKK7123		16 29 35.8	−59 37 47	327.78	−8.08	16x 13	17.4	L ?	13341 240			
WKK7126		16 29 39.2	−61 31 30	326.37	−9.37	34x 19	16.1	SY	10059 193	10128 100	6	*
WKK7138	L137-032	16 30 04.4	−61 56 33	326.09	−9.68	116x 12	15.6	S 5		4511 100	6	*
WKK7140		16 30 11.5	−58 27 38	328.70	−7.34	30x 20	16.3	L ?	5481 136			
WKK7147		16 30 24.9	−62 21 01	325.81	−9.99	31x 26	15.9	S 0 :	5179 121			
WKK7157		16 30 49.0	−61 17 26	326.64	−9.31	51x 13	15.8	S 0	5328 149			
WKK7166	SGC1631	16 31 05.2	−58 06 56	329.03	−7.20	117x 90	13.5	L	1573 86			
WKK7223		16 33 39.0	−61 00 46	327.08	−9.38	67x 23	15.3	S 0	5424 123			
WKK7261		16 35 27.9	−60 17 10	327.78	−9.06	26x 22	15.8	E		5754 70	1 6 7	
WKK7284		16 36 22.7	−59 44 31	328.27	−8.79	22x 9	17.0	F	4813 102			
WKK7290		16 36 32.0	−61 33 03	326.90	−9.99	46x 24	15.6	S 1 :	4937 162			
WKK7304		16 37 20.1	−56 35 09	330.75	−6.80	19x 15	16.9	L ?	14104 126			
WKK7306		16 37 23.7	−54 42 51	332.16	−5.57	95x 65	13.7	E	5111 222			
WKK7324		16 38 11.3	−58 56 40	329.03	−8.44	15x 10	17.3	E	15717 148			
WKK7326	SGC1638	16 38 16.2	−55 50 20	331.40	−6.41	93x 75	13.6	E 1	5066 142			
WKK7357		16 39 44.5	−60 16 19	328.14	−9.46	15x 12	17.3	F	21348 120			
WKK7360		16 39 48.1	−59 24 43	328.81	−8.90	34x 17	16.3	S E	16005 183			
WKK7401		16 41 00.4	−59 49 55	328.58	−9.29	50x 32	15.0	S 1	5496 193	5295 100	6	
WKK7409		16 41 20.1	−58 13 04	329.86	−8.28	22x 12	16.8	F	14364 122			
WKK7420		16 41 48.2	−59 29 38	328.91	−9.15	39x 19	16.2	S 2	[5096] 239			
WKK7465	L137-042	16 43 16.6	−60 03 38	328.59	−9.66	112x 66	13.6	S 4	3480 250	3236 58	3 6 7	*
WKK7471		16 43 29.8	−57 55 50	330.27	−8.31	31x 24	15.9	L	14954 93			
WKK7475		16 43 38.8	−58 02 44	330.19	−8.40	22x 13	16.8	F	14256 140			
WKK7511		16 44 51.4	−60 28 30	328.40	−10.07	22x 10	17.2	F	16149 180			
WKK7522		16 45 07.0	−56 52 26	331.23	−7.80	19x 17	16.9	F	14010 182			
WKK7525		16 45 09.8	−58 30 39	329.96	−8.85	30x 12	16.8	S 0	14940 186			
WKK7548		16 46 03.4	−56 30 32	331.59	−7.67	42x 30	15.6	E	13947 135			
WKK7570		16 46 38.3	−59 48 11	329.07	−9.82	16x 13	16.7	E	13725 194			
WKK7571		16 46 39.7	−59 55 58	328.97	−9.90	42x 22	15.6	F	5954 158			*
WKK7579	L137-046	16 46 47.9	−58 54 28	329.78	−9.27	156x151	12.0	S 3 :		1560 70	3 6	*
WKK7582		16 46 51.2	−59 56 44	328.97	−9.93	23x 12	16.7	E	15206 168			
WKK7615		16 47 35.0	−59 53 44	329.07	−9.97	20x 12	16.9	S P1 ?	15614 183			
WKK7619		16 47 41.9	−59 48 23	329.15	−9.92	48x 15	15.9	S 1	[14461] 250	14651 58	3 6 7	*
WKK7624		16 47 48.9	−59 43 47	329.22	−9.89	17x 16	17.0	E	15978 139			
WKK7628		16 48 00.4	−59 25 44	329.47	−9.72	31x 8	17.1	S E	12386 187			
WKK7631		16 48 03.1	−52 25 20	334.95	−5.28	59x 46	14.6	E	4604 250			
WKK7653		16 48 25.8	−52 29 02	334.94	−5.37	26x 20	16.4	F		4377 70	6 7	
WKK7654		16 48 27.2	−58 35 14	330.17	−9.23	77x 17	15.6	L P		2536 58	6 7	*
WKK7657		16 48 36.2	−59 36 45	329.37	−9.89	55x 30	15.4	L	14460 109			*
WKK7659		16 48 40.4	−59 39 17	329.35	−9.92	20x 12	17.1	S E:	[13727] 250			
WKK7660		16 48 42.1	−59 39 20	329.35	−9.93	23x 15	16.7	L	14683 174			
WKK7688		16 49 27.7	−58 58 03	329.95	−9.57	27x 19	16.6	F	14020 78			
WKK7748		16 51 37.8	−59 19 52	329.84	−10.02	47x 24	15.9	S 1	4823 250	4757 58	1 6 7	*
WKK7876		16 59 07.7	−58 00 35	331.51	−9.98	51x 23	15.8	S 1 :	14526 142			*
WKK7959		17 04 46.1	−52 35 03	336.39	−7.39	19x 19	16.7	L ?	19061 159			
WKK7979		17 05 41.4	−52 40 38	336.40	−7.55	30x 27	16.0	E	19256 250	19123 70	6	
WKK8056		17 09 50.6	−52 44 46	336.72	−8.10	24x 15	16.9	L ?	[18264] 208			
WKK8065		17 10 16.4	−55 20 41	334.61	−9.66	23x 15	17.1	F	17788 202			
WKK8092		17 12 01.4	−52 44 05	336.92	−8.37	28x 17	16.6	S 0 :	[10270] 217			
WKK8115		17 13 45.1	−54 12 08	335.85	−9.42	28x 17	16.6	S E:	18044 127			

Table 2. Partially obscured galaxies in the Great Attractor region for which no redshift could be obtained.

WKK Ident (1)	Other Ident (2)	R.A. (h m s) (3)	Dec. (° ′ ″) (4)	gal ℓ (°) (5)	gal b (°) (6)	D x d (″) (7)	B_J (^{m}) (8)	Type class. (9)	Notes (10)
WKK4376		14 47 58.5	−52 19 23	320.76	6.14	20x 15	17.5	S 0 :	No reliable features
WKK4687		15 07 32.7	−53 46 23	322.66	3.47	23x 19	17.2	E ?	S/N too low
WKK4821		15 15 30.4	−66 13 21	317.05	−7.69	35x 16	16.7	S E	No reliable features
WKK4865		15 19 06.4	−50 36 33	325.84	5.23	19x 16	17.2	E ?	Stellar spectrum (sp.*)
WKK4910		15 21 42.9	−50 40 06	326.16	4.96	22x 15	17.1	F	Stellar spectrum (sp.*)
WKK5261		15 41 42.7	−58 55 29	323.72	−3.44	28x 23	15.9	L ?	Stellar spectrum (sp.*)
WKK5304		15 43 50.3	−61 34 21	322.30	−5.69	32x 20	15.8	L	Stellar spectrum (sp.*)
WKK5326		15 44 46.5	−47 59 33	330.78	4.92	20x 12	17.6	L ?	No reliable features
WKK5591		15 54 30.5	−65 31 25	320.70	−9.50	22x 13	17.0	S E	S/N too low
WKK5650		15 56 03.2	−60 16 52	324.28	−5.63	52x 19	15.6	S M	Stellar spectrum (sp.*)
WKK5817		16 00 47.1	−59 22 03	325.33	−5.33	28x 26	16.2	?	Stellar spectrum (sp.*)
WKK6139		16 08 20.0	−61 22 49	324.66	−7.45	34x 28	15.7	SYP	Stellar spectrum (sp.*)
WKK6145		16 08 24.3	−49 44 38	332.61	1.07	20x 18	16.8	?S E?	Galactic? (sp.*)
WKK6917		16 24 19.6	−60 18 45	326.82	−8.06	23x 9	17.0	L	S/N too low
WKK7101		16 28 51.4	−60 47 42	326.85	−8.80	19x 19	17.1	?S	S/N too low
WKK7347		16 39 10.7	−53 57 52	332.90	−5.27	60x 54	14.6	?	S/N too low
WKK7515		16 44 57.8	−55 26 09	332.32	−6.86	32x 19	16.3	S E	Stellar spectrum (sp.*)
WKK7686		16 49 23.8	−55 50 59	332.40	−7.61	30x 20	16.5	S E	S/N too low
WKK7865		16 58 34.4	−58 04 58	331.40	−9.97	24x 18	16.7	S 1 :	No reliable features
WKK7900		17 00 43.5	−56 20 55	332.99	−9.16	22x 19	16.5	S E?	Stellar spectrum (sp.*)
WKK7954		17 04 40.1	−53 01 18	336.03	−7.63	16x 12	17.1	E ?	S/N too low
WKK8071		17 10 39.6	−54 04 25	335.69	−8.97	28x 16	16.7	F	S/N too low

Table 3. Partially obscured galaxies in the Great Attractor region that were observed before.

WKK Ident	Other Ident	R.A. (h m s)	Dec. (° ′ ″)	gal ℓ (°)	gal b (°)	D x d (″)	B_J (^{m})	Type class.	v_{lit} km s^{-1}		Notes
(1)	(2)	(3)	(4)	(5)	(6)	(7)	(8)	(9)	(10)		(11)
WKK3763	L220-035	13 41 12.7	–52 07 08	311.09	9.66	171x 44	14.4	S 6	3978		1
WKK3795		13 49 44.3	–51 37 15	312.50	9.86	13x 13	17.9	E	14666	70	2
WKK3829		13 55 43.8	–52 03 59	313.30	9.20	51x 12	16.7	S M	4065	70	2
WKK3894	L221-030	14 07 21.8	–51 56 53	315.07	8.81	77x 16	16.1	S	3202	70	2
WKK3991		14 24 06.3	–51 53 49	317.55	8.00	34x 8	18.0	S M	17164	52	3
WKK4091	L222-010	14 31 40.6	–49 12 08	319.70	10.05	58x 31	15.9	I	632	83	4
WKK4131	L222-012	14 35 50.0	–52 00 40	319.19	7.21	73x 55	14.9	S 5	1471	59	3
WKK4144		14 36 49.3	–52 31 40	319.12	6.67	16x 11	18.0		13273	47	5
WKK4145		14 36 57.5	–53 42 22	318.66	5.59	50x 17	16.7	I	2897	37	3
WKK4231	L222-015	14 41 02.8	–49 11 19	321.13	9.44	159x 60	14.2	SY 5 :	2254	10	4
WKK4423	L223-005	14 51 03.4	–47 57 42	323.18	9.81	65x 62	14.9	SBR5	4838		1
WKK4452	JM145221	14 52 21.4	–51 48 38	321.59	6.29	20x 19	17.1	L	4797		6
WKK4495	L223-006	14 55 05.2	–47 30 01	324.01	9.90	316x228	11.8	S P5	1052	9	7
WKK4513	L223-007	14 55 52.3	–48 52 38	323.47	8.63	97x 58	14.5	S L	2758		1
WKK4535	L223-008	14 57 14.2	–51 32 04	322.40	6.18	85x 47	14.9	S 9 :	9839		1
WKK4549	L223-009	14 57 42.2	–48 05 35	324.12	9.17	176x110	13.2	S L	586	4	8
WKK4571		14 58 57.5	–51 00 37	322.89	6.52	15x 9	17.9	F	10579	38	3
WKK4586		15 00 16.4	–50 21 47	323.38	6.98	28x 19	16.7	S 3 :	10421	50	3
WKK4661	L223-012	15 05 51.9	–52 21 55	323.16	4.81	200x 39	14.1	S 3	1283	99	1
WKK4744	L099-002	15 10 38.0	–63 37 10	317.98	–5.21	109x 51	14.2	SY 4	3092		1
WKK4898	L099-004	15 20 43.3	–62 56 58	319.30	–5.24	50x 26	15.6	S P	8779	23	5
WKK4907		15 21 33.5	–48 38 30	327.26	6.66	40x 16	16.9	S 5	10525	70	9
WKK4935	L099-005	15 23 13.8	–63 59 50	318.96	–6.27	177x106	12.8	SB 2	3629	67	3
WKK5034		15 28 08.5	–49 35 28	327.62	5.27	30x 12	17.0	S 3 :	10537	70	9
WKK5186		15 36 36.6	–59 55 42	322.60	–3.85	46x 26	15.5	S 6	5151	70	9
WKK5195		15 37 03.7	–59 49 12	322.71	–3.80	28x 17	16.7	S	5918	70	9
WKK5253		15 41 13.8	–60 50 08	322.51	–4.92	47x 19	15.9	S M	5093	70	9
WKK5260	L099-009	15 41 37.9	–63 09 23	321.12	–6.79	82x 20	15.4	S L	4963		1
WKK5266	L136-002	15 42 05.2	–62 02 04	321.85	–5.93	90x 22	15.0	S 5	4944		10
WKK5354		15 45 42.9	–60 46 16	322.98	–5.20	19x 17	16.9		12916	36	3
WKK5404	L100-001	15 47 56.3	–62 39 40	322.00	–6.84	71x 20	15.3	S 5 :	6450	70	2
WKK5416		15 48 28.5	–58 14 40	324.84	–3.45	24x 9	17.4	I ?	12403	70	9
WKK5435	L136-006	15 49 16.8	–61 32 06	322.84	–6.07	105x 19	14.8	SY M	4473	16	3
WKK5459	L136-008	15 50 05.8	–61 11 34	323.13	–5.87	78x 32	14.5	S 3	4390	150	11
WKK5492		15 51 20.1	–60 47 42	323.50	–5.65	23x 19	16.6	S	10769	39	3
WKK5568		15 53 48.0	–62 44 37	322.47	–7.34	65x 16	15.6	S 3 :	7460	70	2
WKK5581		15 54 09.4	–66 09 21	320.26	–9.96	58x 39	14.8	SB 4 :	9750	70	2
WKK5584	L136-010	15 54 15.5	–60 09 08	324.19	–5.39	73x 43	14.6	SY 5	5027		1
WKK5642		15 55 53.0	–60 58 25	323.81	–6.15	48x 17	15.9	S M	6045	42	5
WKK5669	L100-007	15 56 43.4	–64 39 31	321.46	–9.00	36x 19	15.7	S 1	4869	70	9
WKK5694		15 57 29.9	–61 00 32	323.94	–6.30	66x 38	14.7	S M	3412	36	3
WKK5722	L136-012	15 58 14.2	–61 38 08	323.59	–6.83	203x 78	12.9	S 5	4372	16	3
WKK5738	L100-008	15 58 39.5	–63 58 37	322.07	–8.62	105x 43	14.1	S 5 :	7721		1
WKK5768	L136-016	15 59 31.0	–60 50 26	324.23	–6.34	211x 26	14.0	S 5	5424	9	12
WKK5781		15 59 52.9	–63 33 45	322.45	–8.40	52x 15	15.8	S 3	7390	70	2
WKK5796	L136-017	16 00 07.7	–60 36 01	324.45	–6.20	109x 22	14.6	S 0 :	5260	50	11
WKK5923		16 03 41.1	–59 05 38	325.79	–5.38	50x 28	15.2	S R3	4514	42	5
WKK6005		16 05 46.7	–64 34 40	322.24	–9.59	52x 11	15.8	S E	12000	70	2
WKK6078	L136-023	16 07 16.2	–60 57 07	324.86	–7.05	91x 24	14.5	S 1	4510	150	11
WKK6207	L137-004	16 09 36.9	–60 48 48	325.17	–7.14	52x 17	15.3	L	3410	500	11
WKK6323		16 11 39.4	–64 19 06	322.89	–9.84	28x 19	16.2	S M	7092	70	2
WKK6340	L137-012	16 11 56.8	–61 10 18	325.13	–7.60	67x 38	14.1	S 1	6400	150	13
WKK6353	L100-015	16 12 05.7	–62 34 00	324.16	–8.61	70x 16	15.8	S 5	9900	70	2
WKK6399	L137-014	16 13 00.4	–58 11 21	327.30	–5.54	74x 32	14.7	S M	2740	75	11
WKK6483	L100-018	16 14 29.5	–62 55 55	324.10	–9.07	85x 66	13.9	S 7	3367		1
WKK6594	L137-018	16 16 39.0	–60 22 05	326.11	–7.43	239x 82	12.6	S 7	606		14
WKK6649	L137-019	16 17 33.5	–60 33 04	326.06	–7.63	67x 35	14.3	L	3320	75	11
WKK6654	L100-020	16 17 37.7	–63 25 59	323.99	–9.67	67x 65	14.2	S R1	5160	36	5
WKK6790	L100-022	16 20 52.6	–62 31 26	324.91	–9.30	112x 62	13.7	L	4850	70	2
WKK6831	L137-025	16 21 43.6	–60 24 48	326.52	–7.90	106x 28	14.4	L	5160	75	11
WKK6839	L100-023	16 22 01.2	–63 04 56	324.60	–9.78	190x 87	12.6	SY 4	3835	5	12
WKK6851	L137-027	16 22 22.4	–59 50 38	326.99	–7.56	208x 48	13.5	S 7	1633		1
WKK6991		16 25 54.8	–61 25 57	326.13	–8.97	79x 56	14.3	S E	3332	36	5
WKK7045		16 27 00.2	–55 05 46	330.87	–4.73	28x 9	17.4	S L	10943	70	9
WKK7149	L137-033	16 30 28.6	–60 30 53	327.19	–8.76	98x 83	13.2	S 4	3250	100	15
WKK7163	L137-034	16 31 00.5	–57 58 35	329.13	–7.10	112x 87	13.3	S 4	2747	16	3
WKK7173		16 31 17.4	–61 48 42	326.28	–9.70	32x 7	17.5	S	17912	41	5
WKK7177	L137-035	16 31 23.1	–61 21 51	326.63	–9.41	112x 36	14.3	S 3	4780	75	11
WKK7196	L137-036	16 32 27.6	–60 55 35	327.05	–9.21	86x 24	14.7	S 0	5570	75	11
WKK7248	L137-037	16 34 57.2	–59 47 16	328.11	–8.69	106x 22	14.8	S 3	5430	50	11
WKK7289	L137-038	16 36 28.7	–60 17 52	327.85	–9.17	191x 73	13.1	SYR5	5148		1
WKK7460	L179-013	16 43 07.3	–57 21 07	330.68	–7.90	198x105	12.7	SY L	757	36	5
WKK7588	L138-001	16 46 59.7	–59 09 00	329.61	–9.44	63x 38	14.7	F	2740	50	11
WKK7602		16 47 23.3	–59 20 35	329.49	–9.60	24x 19	16.5	L	14200	70	2
WKK7652	L138-003	16 48 25.4	–59 08 08	329.74	–9.57	302x179	11.2	SY 3	1482		16
WKK7655	L138-004	16 48 29.1	–58 51 48	329.96	–9.41	93x 28	14.4	S 1	2894	56	17
WKK7693	L138-005	16 49 34.5	–58 41 47	330.18	–9.41	120x 97	13.4	E	3000	150	13
WKK7794		16 54 22.4	–58 24 32	330.80	–9.73	51x 44	15.1	SB 4	5854	70	2
WKK7809		16 55 09.1	–58 41 10	330.64	–9.98	31x 26	16.4	S	14630	70	2
WKK7813	L138-012	16 55 30.2	–58 36 51	330.73	–9.97	101x 70	14.0	S M	4698	44	5
WKK7923		17 02 40.4	–55 01 08	334.23	–8.59	23x 10	17.2	S E	17983	40	5
WKK8147		17 16 27.6	–52 32 28	337.47	–8.81	15x 12	17.5	E ?	21313	41	3

Table 4. Central velocity dispersion measurements for 34 galaxies in the Norma cluster.

WKK Ident	Other Ident	R.A. (h m s)	Dec. (° ′ ″)	gal ℓ (°)	gal b (°)	D x d (″)	B_J (^{m})	E(B-V)	Type class.	v_{abs} km s^{-1}		σ_{raw} km s^{-1}	$\log(\sigma_o)$	
(1)	(2)	(3)	(4)	(5)	(6)	(7)	(8)	(9)	(10)	(11)		(12)	(13)	
WKK5764		15 59 20.1	−60 00 40	324.77	−5.70	34x 32	15.1	0.337	E	5028	93	143 (2)	2.149	0.116
WKK5798		16 00 09.9	−60 25 42	324.57	−6.08	39x 24	15.4	0.346	F	5426	151	365 (3)	2.554	0.073
WKK5836		16 01 29.2	−59 32 45	325.28	−5.53	23x 15	16.3	0.331	F	5415	128	197 (3)	2.286	0.151
WKK5868		16 02 09.4	−61 17 11	324.18	−6.88	59x 44	14.5	0.261	F	3330	107	149 (3)	2.166	0.081
WKK5920		16 03 35.3	−60 23 13	324.91	−6.33	39x 39	14.9	0.285	F	4744	109	206 (3)	2.306	0.076
WKK5972		16 04 58.4	−60 23 56	325.03	−6.45	48x 32	14.8	0.256	E	5563	85	186 (3)	2.261	0.075
WKK5986		16 05 18.7	−62 16 39	323.78	−7.87	52x 44	14.6	0.194	F	5569	188	161 (2)	2.200	0.136
WKK5987		16 05 19.5	−60 19 28	325.12	−6.43	34x 32	15.2	0.250	E	4842	231	244 (2)	2.379	0.095
WKK6012		16 05 51.0	−61 08 10	324.61	−7.07	32x 22	15.8	0.262	F	4352	104	83 (3)	1.912	0.102
WKK6019		16 05 57.3	−60 49 43	324.83	−6.85	54x 22	15.1	0.221	F	5615	172	215 (3)	2.327	0.085
WKK6116	L136-024	16 07 52.0	−60 39 17	325.12	−6.88	47x 42	14.6	0.218	E	3909	208	350 (3)	2.536	0.075
WKK6146		16 08 28.4	−59 06 52	326.23	−5.81	55x 38	14.6	0.290	F	5701	112	320 (3)	2.497	0.089
WKK6180		16 09 11.3	−60 52 45	325.09	−7.16	36x 31	15.2	0.212	F	4619	127	245 (2)	2.382	0.147
WKK6183		16 09 12.9	−60 41 46	325.21	−7.03	30x 24	15.6	0.199	E	5845	148	253 (3)	2.395	0.081
WKK6190	L137-003	16 09 18.5	−60 52 19	325.10	−7.16	27x 17	16.0	0.211	F ?	4454	127	125 (3)	2.087	0.091
WKK6198		16 09 30.5	−61 30 20	324.68	−7.64	22x 17	16.1	0.181	E	4687	182	99 (1)	1.989	0.212
WKK6204	L137-003	16 09 35.4	−60 53 04	325.12	−7.19	42x 35	14.9	0.213	F	4678	127	220 (3)	2.335	0.074
WKK6212		16 09 40.0	−60 51 51	325.14	−7.19	28x 19	15.6	0.210	E	3196	95	120 (3)	2.072	0.089
WKK6229		16 09 50.2	−60 43 26	325.25	−7.10	15x 13	16.6	0.202	E	5300	132	177 (3)	2.239	0.079
WKK6235		16 10 00.9	−61 01 04	325.06	−7.33	32x 24	15.6	0.223	E	4067	100	197 (3)	2.286	0.065
WKK6242		16 10 09.9	−60 46 12	325.25	−7.16	28x 12	16.4	0.198	F	5354	250	191 (2)	2.274	0.086
WKK6269	L137-006	16 10 43.0	−60 46 54	325.29	−7.21	90x 63	13.5	0.195	cD	5409	151	411 (3)	2.606	0.064
WKK6305	L137-007	16 11 13.0	−60 32 24	325.50	−7.08	59x 44	14.4	0.262	E	5038	124	295 (3)	2.461	0.076
WKK6312	L137-008	16 11 25.2	−60 47 38	325.34	−7.28	110x 95	13.1	0.193	cD	3907	132	379 (3)	2.570	0.047
WKK6318	L137-010	16 11 29.6	−60 40 41	325.43	−7.20	121x 82	13.2	0.227	E	3419	182	295 (3)	2.462	0.089
WKK6431		16 13 35.7	−60 48 02	325.53	−7.47	35x 22	15.7	0.239	F	3494	124	191 (2)	2.272	0.120
WKK6473		16 14 22.5	−60 10 21	326.04	−7.09	17x 11	17.0	0.217	E	5561	112	146 (3)	2.156	0.130
WKK6555		16 15 52.6	−60 53 34	325.67	−7.73	28x 17	16.3	0.217	F	4927	167	226 (3)	2.345	0.086
WKK6586		16 16 29.3	−60 58 07	325.67	−7.84	46x 33	15.0	0.202	F	6389	151	156 (3)	2.186	0.089
WKK6679		16 18 11.8	−60 55 13	325.85	−7.95	26x 24	15.9	0.238	E	4598	103	137 (3)	2.128	0.081
WKK6765		16 20 15.6	−61 06 17	325.89	−8.26	47x 34	15.0	0.210	F	5191	124	230 (3)	2.355	0.081
WKK6808	L137-024	16 21 27.7	−60 38 20	326.33	−8.04	85x 70	13.7	0.193	F	5154	167	250 (2)	2.390	0.098
WKK6821		16 21 38.3	−60 28 46	326.46	−7.94	26x 12	16.4	0.196	E	5557	167	140 (2)	2.139	0.130
WKK6870		16 22 57.6	−59 57 42	326.95	−7.70	20x 19	16.3	0.223	E	5488	148	95 (2)	1.970	0.159